Activation of the transcription factor HIF-1 by HMGN1 in Acute Myeloid Leukaemia

Maria Abril Arredondo Garcia

Master of Science by Research (MSc by Research)

University of York

Biology

May 2023

Abstract

Acute myeloid leukaemia (AML) is a disorder in the hematopoietic stem cells causing an overproduction of myeloid stem cells in the bone marrow. The causes of AML remain poorly understood; however, it has been identified that AML is predominantly driven by particular genetic mutations, with only a small percentage due to other factors. The High Mobility Group N (HMGN) is a family of proteins that bind nucleosomes and modulate transcription by opening the chromatin structure for transcription factors (TFs), such as Hypoxia-Inducible Factors (HIF). HIFs are a family of TFs that were originally identified as being activated in the absence of oxygen (hypoxia). HIF-1 is the best characterised of the HIF family, and its activity has been linked to AML disease progression. HMGN1 overexpression is observed in AML, and its knockout reduces leukaemia progression and improves disease phenotype. Our lab identified by CRISPR/Cas9 genome-wide screening that HIF-1 transcription activity is upregulated by HMGN1. This study aims to determine the mechanism by which HMGN1 regulates HIF-1 transcription activity and to identify the contribution of HIF-1 in the pathogenesis of HMGN1-driven AML. Lentivirally transduced inducible knockdown/ overexpression HMGN1 leukaemia cell lines were generated and validated by Western Blots and RT-qPCR. The effect of HMGN1 on HIF-1 activity was assessed in these cells and in combination with HIF-1 inhibitors, using viability assays and CFU assays. Our results demonstrate that HIF-1 activity is regulated by HMGN1 in a panel of AML cell lines and indicate the contribution of particular driver mutations within this transcription activation axis.

Table of Contents

List of Tables

List of Figures

Declaration

I declare that this thesis is a presentation of original work, and I am the sole author. This work has not previously been presented for a degree or other qualification at this University or elsewhere. All sources are acknowledged as references.

Acknowledgements

Words cannot express my gratitude to my supervisor Dr Katherine Bridge, for all the guidance, help and feedback she has given me throughout my project. I would also like to thank the members of the Bridge Lab who gave me a helping hand when things went wrong and shared their knowledge with me.

Also, I want to highlight the support my family gave me during this project and their encouragement and belief in me during this degree.

1. Introduction

1.1 Acute Myeloid Leukaemia

Acute myeloid leukaemia or AML is a disorder in the hematopoietic stem cells affecting the myeloid lineage, the progenitor of red blood cells, platelets and certain white blood cells [1,2].

Different factors that can promote AML have been identified. A minority of cases are caused by chemotherapy or chemical exposure whilst the majority of AML cases are caused by genetic alterations that can be either chromosomal abnormalities or isolated gene mutations. Many of these aberrations have no known cause [1,3]; however, these molecular prognostic markers are important to evaluate as they are used as tools for risk stratification [1,2].

According to Prada-Arismendy et al. [2], epigenetic regulation plays an important role in the early stages of leukemogenesis and the development of AML. Epigenetic modifications that have been identified in AML include DNA methylation, post-translational histone modifications and chromatin remodelling [2].

1.2 AML driver mutations

A number of genetic mutations are frequently observed in AML patients as drivers of this disease. A common mutation driver observed in AML is chromosomal translocation, whereby an abnormal fusion of proteins involved in growth and differentiation pathways creates a proto-oncogene [2]. Within this list of frequently occurring driver mutations in AML are FLT3, K/NRAS, TP53, DNMT3A, NPM1, TET2, MLL, and CEBPA [2,3].

1.2.1 Point mutation-induced oncogenes

FLT3 is a membrane-bound receptor that is expressed in haematopoietic progenitor cells that regulates differentiation and proliferation [2]. This receptor promotes a

cascade of phosphorylation reactions triggering pathways that regulate cell differentiation, proliferation, apoptosis, and cell survival [2]. The mutation present in AML is FLT3-ITD (internal tandem duplication), which is a replicated sequence in the juxta membrane domain of the FLT3 receptor, this mutation results in a constitutively activated FLT3 promoting proliferation and survival in AML cells [4]. This mutation is one of the most common in AML patients and is associated with poor prognosis [4].

Another AML mutation is *NPM1*, a gene that encodes for a protein that has several functions including ribosomal protein assembly and transport and regulation of the tumour suppressor ARF, also it responds to stress stimuli such as hypoxia [2,5]. The NPM1c mutation is been known to block myeloid differentiation, promote cell proliferation and impair DNA damage repair [5]. This mutation is considered an encouraging prognosis for patients; however, most of them would relapse [5].

TP53 is a DNA-binding protein that works as a tumour suppressor, and it induces cell cycle arrest, apoptosis and DNA repair [2]. This is considered the most common mutated gene in cancer [6]. TP53 is involved in multiple transduction pathways allowing the regulation of several cellular processes, including genomic stability, cell cycling, proliferation, differentiation, apoptosis, senescence, autophagy and stem cell homeostasis [6].

1.2.2 Molecular mutations that induced AML

MLL protein is a histone methyltransferase that regulates transcription and is important for haematopoiesis as it is critical for the development of the erythroid and megakaryocytes lineage [2,7]. Its role as an oncogene occurs when it gets fused with AF4, AF9, ENL, AF10 or ELL[2]. The chromosomal translocations in MLL that lead to AML are known to signify poor prognosis in patients [7].

A missense somatic mutation on the RAS pathway gene is *NRAS* [8]. *RAS* gene encodes for the G protein family that induces proliferation, differentiation and apoptosis [2]. When mutated they drive oncogenesis by increasing cell survival and proliferation [8]. It has been shown that RAS mutations are needed for driven

oncogenesis but also for tumour maintenance [8,9]. This mutation usually refers to a poor prognosis when in combination with another mutation [9].

1.2.3 Epigenetic mutations drivers of AML

DNMT3A is involved in DNA methylation and gene silencing and also helps with haematopoietic stem cell renewal and myeloid differentiation [2]. Abnormal DNA methylation contributes to cancer pathogenesis [10]. It is considered that in some cancers this mutation causes hypermethylation in promoters of tumour-suppressor genes[10]. This mutation is common in AML patients and is associated with poor prognosis and survival [10].

Most of those mutations can be found separately on AML cell lines. Table 1 shows the main mutations found on the AML cell lines that would be explored in this study.

Cell line	Classification	Oncogenic Alterations
K562	Chronic Myeloid Leukaemia	BCR-ABL1+[11] TP53- Loss of function[11] ASXL1- Loss of function[11]
HL-60	Acute Myeloid Leukaemia	NRAS- Gain of function [12] CDKN2A- Loss of function [12] MYC- Amplified[13]
MOLM-13	Acute Myeloid Leukaemia	FLT3- Gain of function [14]
OCI-AML3	Acute Myeloid Leukaemia	NRAS- Gain of function [15] NPM1- gene mutation [16] DNMT3A R882C- mutation [16]
THP-1	Acute Myeloid Leukaemia	NRAS- Gain of function [17] TP53- Loss of function [17] T(9;11)(p21;q23) KMT2A- MLLT3- AF9 fusion gene [18]

Table 1. Mutations present in the AML cell lines used in this study.

1.3 Hypoxia and the Hypoxia-inducible Factor (HIF)

Hypoxia refers to the state of low oxygen levels and is commonly found in the tumour environment as a driver for malignancy. It is related to the aggressiveness, metastasis rate and resistance to therapy in the cancer cells. The response to a hypoxic environment is achieved via the signalling pathway of the HIF transcription factors [19]. Hypoxia in tumours can be chronic (inadequate oxygen supply) or acute (fluctuation of oxygen levels)[20].

Hypoxia-Inducible Factors (HIFs) are markers of tumour hypoxia and their expression is increased in hypoxic environments, which are linked to genomic instability, genetic alterations, mutagenesis and poor prognosis [20]. The HIF family has three oxygen-sensitive isoforms: HIF-1α, HIF-2α and HIF-3α and the oxygen-insensitive HIF-1β, which forms a heterodimer with the HIF-1α subunits [19,20]. The most characterised member and the one more relevant for this project is HIF-1. HIF-1α is a transcription factor that is regulated according to certain conditions whilst HIF-1β is an active transcription factor independent of the conditions; additionally, the HIF-1α protein gets degraded in normoxic conditions by the ubiquitin-proteosome system whilst HIF-1β protein is always stable in hypoxic or normoxic conditions [20].

HIF-1 is made up of different functional domains: the DNA binding domain is formed by a basic helix-loop-helix (bHLH) domain that with the addition of the PAS domains becomes the heterodimerization domains between HIF-1α and HIF-1β [20]. Additionally, HIF-1 has a transactivation domain (TAD) on the c-terminal side, which regulates the transactivation of the target genes via co-activator recruitment [20] (Figure 1).

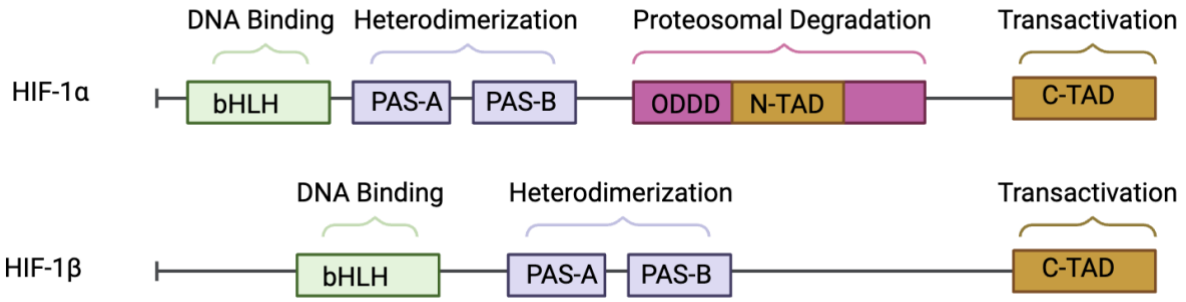

Figure 1. Diagram of the functional HIF-1 domains in HIF-1α and HIF-1β. Diagram shows the DNA binding domain formed by basic Helix-loop-helix (bHLH), the heterodimerisation domains PAS, the oxygen-dependent domain (ODDD) which is for HIF-1α only and the transactivation domains (TAD). Diagram made with BioRender.

In HIF-1α, there is an oxygen-dependent degradation domain (ODDD) which gets hydroxylated by proline-hydroxylase-2 (PHD-2) [21]. PHD-2 and Von- Hippel-Lindau (VHL) are ubiquitin ligase complexes that allow degradation in normoxia [21]. While PHD-2 is activated by HIF-1 creating a feedback inhibition, VHL proteins are stable hydroxylases and are inhibited by the absence of oxygen [21].

When oxygen concentrations are limited, it decreases HIF-1α hydroxylation, accumulating it in the cytoplasm, which is translocated to the nucleus and dimerizes with the HIF-1β subunit. The HIF dimer interacts with the hypoxia response elements (HREs) that can be found in the promoters' oxygen-dependent genes that encode proteins involved in systematic and cellular adaptation to hypoxia [19] (Figure 2). The HIF target genes are known to contribute to angiogenesis, cell survival and tumour aggressiveness [22]. The main genes that HIF-1α promotes transcription of are the genes involved in angiogenesis including VEGF [23].

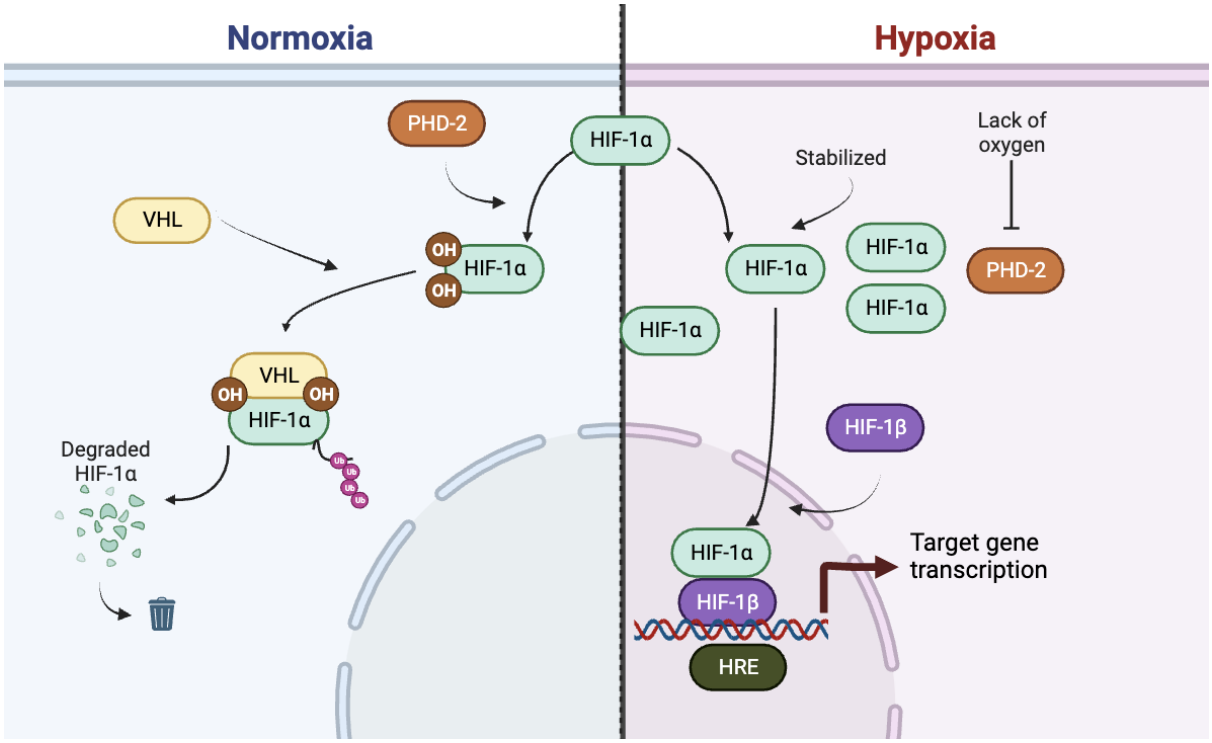

Figure 2. Diagram showing the mechanism of action of HIF-1. HIF-1α in normoxic conditions degrades by PHD-2 hydroxylating the HIF-1α subunit and then binding with VHL and the ubiquitin ligase complexes so that HIF-1α can be degraded. Also shows the hypoxic conditions where HIF-1α is able to heterodimerise with HIF-1β and go to the nucleus to interact with HREs to promote gene transcription. Diagram made with BioRender.

HIF-1/2 expression contributes to mortality in cancer patients; these transcription factors activate genes encoding proteins that drive vascularization, immune evasion, metabolic reprogramming, growth factor signalling, tumour progression and metastasis[19,20]. It has been found that many cancers including breast, myeloid leukaemia, liver, ovarian and others tend to respond poorly to treatments due to HIF activation [19,20]. Additionally, HIF activation during tumour progression can determine the development and outcome of the disease [19].

1.4 HIF role in AML transcription of proto-oncogenes and tumour suppressors

Hypoxia is known to play a crucial role in cancers as HIF controls the transcription of a wide array of genes including both proto-oncogenes and tumour suppressors [19]. Research on the contribution of HIFs to AML disease progression has demonstrated highly context-dependent results.

It has been suggested that HIF-1 in AML supports the disease progression as an oncogene [24]. Additionally, it has been shown that constitutive expression of HIF-1α in AML is associated with poor prognosis as AML cells benefit from the hypoxic microenvironment in the bone marrow [25]. It is believed that the excess proliferation and accumulation of cells in AML in the bone marrow cause a hypoxic environment for cancer cells[24].

It has been demonstrated that HIF-1α regulates pro-leukemogenic functions such as bone marrow angiogenesis and cell migration [26]. It is considered that tissue-level hypoxia can help select cancer cells that are resistant to apoptosis [27]. Nonetheless, it seems that the research done so far suggests that HIF-1's role in AML is context-dependent [26].

1.5 HMGN1

High Mobility Group N (HMGN) is a family of proteins that bind nucleosomes and can affect chromatin structure [28]. This family is comprised of five different proteins (HMGN1-5) [28]. This family is characterised by having a highly conserved nucleosome binding domain [29]

HMGN proteins play an important role in embryogenesis, can affect cell differentiation and are involved in DNA repair processes [28]. Also, the loss of the HMGNs can lead to cancer and neurological disorders and alter immune functions [28]. It has been suggested that the relative levels of HMGN during early embryogenesis might implicate a role for HMGN proteins within lineage commitment and cellular differentiation, with HMGN1 being found in high levels within embryonic stem cells and induced pluripotent stem cells [28].

HMGN proteins have been shown to modulate the interaction of DNA repair factors with the chromatin [28]. HMGN1 interacts with the H3 tail and DNA near the dyad axis of the nucleosomes [30]. When it is bound to the nucleosomes, HMGN1 impacts the

chromatin through a less conserved regulatory domain that is enriched with negatively charged residues [30].

HMGN1 encodes a nucleosome-binding protein that modulates transcription and promotes chromatin decompaction; it competes with histone H1 for binding to the nucleosome for histone post-translational modifications [31–34], this competition caused HMGN1 to counteract H1- mediated transcription inhibition [29]. HMGN1 and the HMGNs in general as previously stated are known for binding to the nucleosome and reducing the compaction of the chromatin fibre, changing the chromatin structure [28]. However, it has been found that HMGN1 preferentially localises to DNase I hypersensitive sites, promoters functional enhancers and transcription factor binding sites, which are associated with chromatin regulation and active transcription [29,35].

It has been studied that the changes in the levels of HMGN1 can influence modifications in gene expression and cause up or down-regulation of tissue-specific gene expression [28,36]. It has been shown that HMGN1 knockout reduces leukaemia progression and improves some of its phenotypes such as hepatosplenomegaly, anaemia and thrombocytopenia [37]. Also, it has been shown that HMGN1 could be influencing both post-translational modifications and mRNA expression [32].

It has been demonstrated that the deletion of HMGN1 can inactivate histone and chromatin activity [35]. Also that HMGN1 can relax chromatin compaction and modify it but it would not initiate transcription on its own [33].

Research has been done regarding the function of HMGN1 and in solid tumours it has been shown that extracellular HMGN1 can act as an alarmin, a mediator that can induce immune response [38]. The experiments were done to determine where the extracellular HMGN1 that acts as an antitumour came from, results from the bone marrow showed that the cells of haematopoietic origin were not capable to do that [38].

Additionally, it has been demonstrated that HMGN1 can play a driving role in haematological malignancies [32], where HMGN1 binds to specific gene regulatory elements in promoter regions to modulate gene regulation interacting with transcription

factors, this lead to consider that HMGN1 is important for leukaemia development and not progression [32].

1.6 HMGN1 is a known leukaemic driver

HMGN1 is located on chromosome 21 in a region known as the Down's syndrome (Ds) critical region (DsCR), and for both Ds human cells and the Ds mouse model, an elevated HMGN1 expression there has been found in these [28].

Ds is caused by a trisomy of chromosome 21 due to nondisjunction during meiosis[32,39], the extra chromosome is associated with cardiac defects, growth abnormalities, endocrinopathies and learning disabilities. Moreover, Ds patients are heavily associated with leukaemia as they are known for being born with a transient myeloproliferative disorder known as pre-leukaemia [28,32,33,39,40].

The specific gene from chromosome 21 that can affect and promote leukaemia in a Ds patient is unclear and it is thought that the two main genes that could be implicated are HMGN1 and DYRK1A [40]. The gene HMGN1 is located not only on chromosome 21 but also in the region that is commonly triplicated to induce Ds, it has been discovered that the mouse model of Ds expresses 1.5 times more HMGN1 mRNA and protein than the Wild-type [28]. There seems to be a direct correlation between HMGN expression and a human phenotype in Ds, in patients with an increase of HMGN1 it also shows an increased incidence of leukaemia [28].

Part of the relationship between Ds and HMGN1 consists of Ds cases where there is an overexpression of the HMGN1 mRNA and protein that could increase the chromatin accessibility and cause transcriptional dysregulation [35]. It has been shown that there is an overexpression of HMGN1 in patients with Ds and that HMGN1 is essential for the B cell phenotype in the Ds models [33]. It is known that the trisomy of chromosome 21 is related to a high incidence of acute leukaemia in Ds patients. A set of experiments showed that in Ds cells there is an alteration in gene expression and histone modifications across all chromosomes, this makes us believe that chromosome 21 and especially the trisomy modulate gene regulation [33].

One of the hallmarks of cancer is transcriptional addiction and HMGN1 overexpression due to the chromosomal trisomy is considered to contribute to leukaemia as it enhances the transcription; additionally, with increased transcriptions, it means that there is an increased activity of survival pathways that could overcome growth-limiting conditions [33]. Where there is an increase of transcriptional amplification this can become oncogenic as it enhances multiple growths and survival phenotypes and it has been identified on transformed cells and increased RNA output, this RNA increases when mediated by HMGN1 they can improve the survival of a leukaemia cell [33].

Mouse models with trisomy in the equivalent of human chromosome 21 show myeloproliferative disorder [40]. It has been suggested that HMGN1 is one of the critical genes in mice needed for cell self-renewal [33,40]. Some studies had highlighted the role of trisomy 21 in leukaemia both in the predisposition for the disease and how it will develop later in life [39].

The trisomy of chromosome 21 is associated with AML but the specific gene responsible for that is not fully known or understood, though the amplification caused by the trisomy has been linked to the abnormalities in the myeloid differentiation and HSPC functions that are mediated by HMGN1 [34]. The effect of HMGN1 in cellular differentiation is dependent on the residues necessary for the binding to the nucleosome and are required for the chromatin modification [34].

It has been shown that HMGN1 binds to specific gene regulatory elements in promoter regions to modulate gene regulation and interact with transcription factors, with this it can be suggested that HMGN1 has more impact in leukemic development rather than progression as it has been previously stated [32].

1.7 Preliminary data

Dr Katherine Bridge conducted a CRISPR library screen on the HIF-1 reporter cell line A549, an adenocarcinoma cell line, to identify novel HIF activity regulators. Then the

reporter line A549 was transfected with the GECKO library which collectively targeted 19050 genes, as the readout of the cell line was with GFP, they were sorted by GFP expression. The cells with a significant reduction or enhancement of the GFP expression would indicate that a gene has been targeted and that it can regulate HIF activity.

Afterwards, genomic DNA sequencing was performed, and 18 genes were identified as novel regulators of HIF. CRISPR editing of HMGN1 caused a reduction in HIF-1 transcription activity, identifying a putative role for HMGN1 as a transcriptional enhancer of HIF-1 activity. This result was validated in the cell line where the initial screen was done (A549) to assess whether HMGN1 could regulate the gene activity. A knockdown was performed, and the RNA was run in an RT-qPCR panel of 89 HIF target genes. Given the high relevance of HMGN1 in AML, this project sought to validate this finding within the setting of AML disease.

1.8 Aims

The aim of this project is to validate HMGN1 as a regulator of HIF-1 transcription activity and identify the contribution of an HMGN1/HIF-1 axis within AML disease.

2. Methods

2.1 Cell culture

K562, HL-60 and HEK 293 LentiX (Bridge Lab) and OCI-AML3, MOLM-13 and THP-1 gifts from Grey Lab. For routine culture, K652, HL-60, OCI-AML3, MOLM-13 and THP-1 were maintained in R10 media as it contained: RPMI 1640, no glutamine (Gibco 31870025), supplemented with 10% Foetal Bovine Serum (ThermoFisher A4766), penicillin-streptomycin (Gibco 15140130) and L-glutamine (ThermoFisher 25030081). Transduced cells that were induced by doxycycline were supplemented with 10% Fetal Bovine Serum Tet System approved (ThermoFisher A4736401).

HEK 293 LentiX cells were maintained in DMEM (Gibco 2196035) supplemented with Fetal Bovine Serum. All cell lines were grown in a 37°C humidified incubator with 5% CO_2. For hypoxic exposure, cells were incubated in a hypoxic chamber (Biospherix, ProOC Oxygen Single Chamber P110) at 1% O_2. Cells were routinely passaged every 2-3 days as required.

2.1.1 Cell Seeding

For drug treatment assays, cells were seeded at a density of $1x10^5$ per well in 2 ml of complete media. Doxycycline (DOX) treatment was administered at a final concentration of 0.05μg/mL in RPMI 10% FBS Tet System approved. Cumate (CMT) induction was performed with a final concentration of 30 μg/mL in RPMI 10% FBS. Cells were incubated for 72 hrs post-induction.

2.1.2 Cell Transfection and Transduction

HEK 293 LentiX were seeded at $1x10^6$ cells per well of a 6-well plate with 2ml of DMEM complete media incubated overnight. The following day, cells were transfected with 2μg of DNA in optiMEM in a total volume of 100μl and 20 μl of PolyFect Transfection Reagent (QIAGEN, 301105) according to its manufacturers' protocol, in fresh DMEM media. Cells were incubated overnight and the following morning, 3ml per well of fresh DMEM media was replaced.

48hrs post transfection, the supernatants of the wells were recovered and filtered with a syringe. To the lentiviral supernatants, 10μg/ml of Polybrene was added. $1x10^5$ cells per well were transduced with about 2.5ml of lentiviral supernatant and incubated overnight. The following day, cells were washed with 1x PBS and fresh RPMI medium was replaced (RPMI with Tet system approved for knockdown). Transduced cells were left to recover for 24hrs prior to selection by puromycin at the optimum determined concentration for each cell line.

Two different lentiviral constructs were used to transfect the different cell lines. The shRNA HMGN1 construct was made by Dr David Kealy in Bridge Laboratory. The

backbone pLKO-Tet-On (Appendix 2) used was a gift from Prof. Tyson Sharp to Bridge Lab though it was originally generated by Dmitri Wiederschain [41,42]. The HMGN1 sequences were chosen by Dr Kealy (Appendix 3) and then he requested the oligo with the additional sequences required from integrated DNA technologies.

The HMGN1 overexpression construct was made by me with the advice of Dr David Kealy, the system was made using the SBI SPARQ Cumate Switch System (Appendix 1), The HMGN1 sequence was amplified from K562 cDNA.

2.2 Western Blot

2.2.1 Protein extraction

For protein extraction from cell culture, cells were pellet by centrifugation at 1000xg for 1 minute, washed with 1mL of 1x PBS and Protease Inhibitor (Roche 04693159001, 1 tablet dissolved in 10 mL PBS) and lysed by the addition of 1x Cell Lysis Buffer (16% SDS powder, 60% glycerol, 300mM of Tris pH 6.8 and bromophenol blue) with 1% 100x Protease and Phosphatase inhibitor cocktail (ThermoFisher 78441), 0.1% MG132 inhibitor, nuclease-free water and 6.8% β- mercaptoethanol. For every well of a 6-well plate 75ul of lysis buffer was used. Samples were incubated on ice for 5 minutes and then vortexed prior to boiling for 10 minutes at 95°C.

2.2.2 Western Blotting

Samples were resolved using 4-20% polyacrylamide precast gels (Mini-protean TGX Satin-Free Precast gels, Bio-Rad 4568094), run at 100V for 85 minutes. Protein size was determined using a molecular weight marker (Precision Plus Protein All Blue Prestained Protein standards, Bio-Rad 1610373).

Gels were transferred to a PVDF membrane using a Semi-Dry Trans-Blot Turbo system (Bio-Rad 1704150). Membranes were then blocked for 10 minutes using EveryBlot blocking buffer (Bio-Rad 12010020). Membranes were incubated with the appropriate primary antibody in 5% milk in TBS overnight at 4°C. Membranes were

washed 5 times for 5 minutes with TBS-T before proceeding to secondary antibodies incubation for 1 hour with 5% milk powder in TBS/ 0.02% SDS. Membranes were washed 6 times for 5 minutes with TBS-T and imaged using the ChemiDoc MP imaging system from Bio-Rad.

Protein	Antibody Source	Species	Dilution factor
HMNG1	Cell Signalling Technology #5692	Rabbit	1:1000
HIF 1α	Cell Signalling Technology #36169	Rabbit	1:1000

Table 2. Primary antibodies used in western blots.

Antibody Name	Antibody Source	Species	Dilution factor
StarBright Blue 700 anti-Rabbit	Bio-Rad #12004162	Goat	1:2500
hFAB Rhodamine anti-actin	Bio-Rad #12004164	Human	1:5000

Table 3. Secondary antibodies used in western blots. Although, anti-actin is a primary antibody it was used during the secondary antibody incubation.

2.3 RT-qPCR

2.3.1 RNA extraction

RNA extraction was performed using either illustra RNAspin Mini RNA Isolation Kit (GE Healthcare #25-0500-72), or Monarch Total RNA Miniprep Kit (New England Biolabs #T2010S), according to the manufacturers' protocol. RNA was eluted in 100μl of nuclease-free water.

2.3.2 Reverse Transcription (RT)

Reverse transcription was performed using either SuperScript IV VILO Master Mix with ezDNase Enzyme (ThermoFisher #11766050), or Luna Script RT SuperMix Kit (New England Biolabs #E3010), according to the manufacturers' protocol. 1μg of RNA was used and at the end diluted 1:5 to perform RT-qPCR.

2.3.3 RT-qPCR

Quantitative real-time PCR was performed. To set the reactions each of them contained, 2μl of cDNA of the desired sample and 18μl of the master mix that contained: forward and reverse primer of interest (Table 3) and SsoAdvanced Universal SYBR Green Supermix (Bio-Rad #1725270).

Target transcript	Forward primer	Reverse primer
HIF-1α	GTACCCTAACTAGCCGAGGAAGAA	GTGAATGTGGCCTGTGCAGT
HMGN1	GATGCCCAAGAGGAAGGTCAG	CAGCAGCGAAGGATAAATCTTC
VLDLR	AGTATGTAACCAGGAGCAGGAC	CACAGTCACACTCGTAGCCTAT
VEGFA	ATGACGAGGGCCTGGAGTGTG	CCTATGTGCTGGCCTTGGTGAG
MIF	CATCGTAAACACCAACGTGC	CCGCGTTCATGTCGTAATAG
LDHA	GGTTGGTGCTGTTGGCATGG	TGCCCCAGCCGTGATAATGA
GLUT1	GAGCCTGAGCGGGAGAGC	GACCCGTCAGCTTCTTGC
CDKN1A	CGATGGAACTTCGACTTTGTCA	GCACAAGGGTACAAGACAGTG
CA9	CATCCTAGCCCTGGTTTTTGG	GCTCACACCCCCTTTGGTT
RPLP1	AGCCGGTGTAAATGTTGAGC	CAGATGAGGCTCCCAATGTT
RPL30	ACAGCATGCGGAAAATACTAC	AAAGGAAAATTTTGCAGGTTT

Table 4. Sequences of primers used for real-time PCR.

2.4 Cell Viability Assays

2.4.1 Trypan Blue

To determine the percentage of life and dead cells, the viability was assessed using Trypan Blue Stain (0.4%) (ThermoFisher #T10282) by a Countess II Automated cell counter (ThermoFisher). Viability analysis was performed using GraphPad Prism.

2.4.2 RealTime-Glo MT Cell Viability Assay

For longitudinal cell viability assays, cells were seeded at a concentration of $1x10^5$ cells per well in a 6-well plate with either doxycycline or cumate for 72hrs. Cells were then washed with 1x PBS and resuspended in complete media.

$7.4x10^4$ cells were then seeded per well of a 96-well white flat-bottom plate (Falcon #353296) in complete media plus 1x RealTime-Glo master mix (Promega #G9713), with or without the addition of 30μg/ml of cumate, 0.05μg/ml of doxycycline and/or 1μM final concentration of the HIF-1α inhibitor GN44028.

Viability was assessed by the bioluminescence emission at time points 0hrs, 24hrs, 48hrs, 72hrs and 96hrs using the CLARIOstar plate reader. Analysis of cell viability was performed using GraphPad Prism.

2.4.3 Drug treatments for viability assay

Cells were seeded at a density of $1x10^5$ cells per well in a 6-well plate with R10 media and a range of puromycin concentrations to determine the optimal concentration for the different cell lines. A dose curve of puromycin was applied to each cell line (0μg/ml, 0.25μg/ml, 0.5μg/ml, 1μg/ml, 2μg/ml and 4μg/ml), and the following concentrations were deemed optimal for each line.

Cell line	Optimal Puromycin Concentration
HL-60	1μg/ml
MOLM-13	0.5μg/ml
THP-1	0.5μg/ml
OCI-AML3	0.5μg/ml

Table 5. Final optimal concentrations of puromycin used.

2.5 Colony Formation Unit Assay

All steps were performed under sterile conditions in cell culture hoods.

2.5.1 Preparation of media

Methocult (Stem Cell Technologies #H4435) and StemSpan SFEM II (Stem Cell Technologies #9655) were used to prepare methocult media in 15 ml falcons using a blunt-end 16-gauge needle with a 5 ml syringe. Each tube contained 5 ml of methocult. Aliquots not needed would be kept at -20°C.

2.5.2 Plate preparation

Meniscus-free Smart Dishes (Stem Cell technologies # 27371) were prepared by the addition of 750μl of tissue culture grade, sterile ddH_2O in the spaces between the wells of the plate.

2.5.3 Sample Preparation

After induction, cells were washed with 1x PBS, resuspended in 1ml of StemSpan and counted. 1.5 ml tubes were labelled with each sample name, 2500 cells per replicate were added and topped up StemSpan to have 250μl per technical replicate (750μl total), plus/minus HIF-1α inhibitor and DOX/CMT, as required.

Cell suspensions were added to prepared methocult, and falcons were vortexed to produced homogenous suspension. Suspensions were left to stand for at least 10 min to allow any bubbles to rise to the top of the media before plating. A blunt-end 16-gauge needle with a 5 ml syringe was used to dispense approximate 2.5 ml of suspension into each well, taking care to not draw any bubbles. Plates were incubated for 10 days in either a highly sensitive culture incubator or under hypoxic conditions.

2.5.4 Imaging the plates

Plates were imaged on days 0, 2, 4, 7 and 10 using Stem Vision System and its acquisition software (Stem Cell Technologies). Images were acquired using the settings “Human 14-day assay” and analysed using the colony counter feature in ImageJ.

2.6 Statistical Analysis

2.6.1 Western Blot

The western blot membranes were analysed and semi-quantified using the Analyse gel function. The results were normalised to the Actin levels loaded.

2.6.2 Cell viability

Cell viability was measured with the Countess II Automated cell counter. Then the percentage of life cells was plotted using GraphPad Prism.

For the RealTime Glo viability assay, the bioluminescent data was normalised to its control (no drug no induction) at times 0hrs and 48hrs, After the normalisation it was plotted in GraphPad Prism. The statistical analysis performed was the two-way ANOVA test.

2.6.3 RT-qPCR

Was analysed using the ΔΔCt method. The values were then plotted in GraphPad Prism and the statistical analysis performed was the two-way ANOVA test.

2.6.4 Colony Formation Assay

The plates with the colonies were scanned using STEMvision. Images were analysed for colony count with ImageJ, colony counter function. To compare the data a two-way ANOVA test was used.

3. Results

3.1 HMGN1 in AML cell lines

First, to characterise the function of HMGN1 in AML cell lines with different driver mutation status, the protein levels of HMGN1 were analysed. Western blot analysis was performed upon cell lysate from cells cultured in normoxic (20% O_2) or hypoxic (1% O_2) conditions for 4 hours. Equalised loading was confirmed by western blot of β-Actin, and densitometry of HMGN1 was performed normalised against β-Actin.

Under normoxic conditions, HMGN1 protein levels were highest in HL-60 cells, followed by K562, with OCI-AML3 and THP-1 demonstrating the lowest protein levels comparatively (Figure 3A). Interestingly, MOLM-13 cells did not have any detectable HMGN1 proteins. Under hypoxia, the protein levels of HMGN1 were dramatically reduced in all 4 AML cell lines (HL-60, MOLM-13, OCI-AML3 and THP-1); however, in the CML line K562, HMGN1 protein levels increased by 1.7-fold.

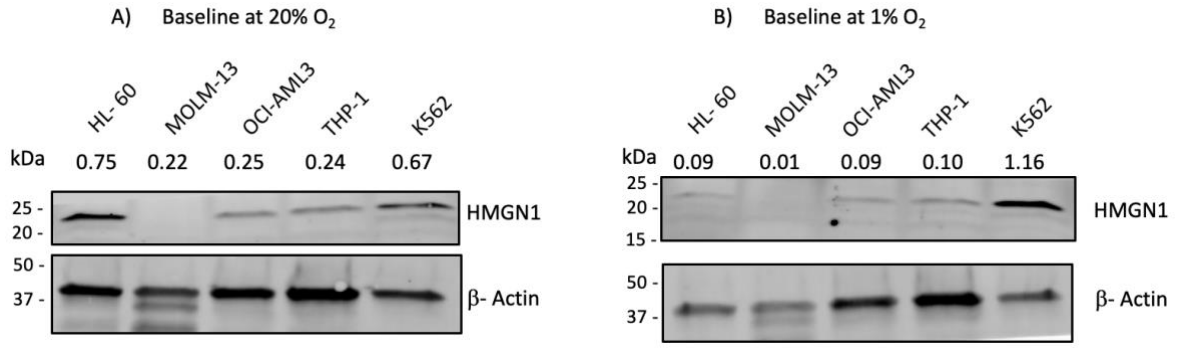

Figure 3. Protein levels of HMGN1 in a panel of myeloid leukaemia cell lines. Western blot analysis of HMGN1 in the indicated cell lines cultured under A) normoxic conditions (20% O_2), 45µg lysate or B) hypoxic conditions (1% O_2, 4 hours), 60µg lysate. β-Actin loading control. Densitometric values displayed are of HMGN1 bands normalised against β-Actin. Image representative of n=2.

Next, proteinatlas.org [43] was used to interrogate the expression levels of HMGN1 from RNA-seq datasets in the cell lines included in this study. These analyses demonstrated that HL-60 had the highest HMGN1 transcript expression levels of the panel, with 1059.8 normalised Transcripts per million (nTPM), and was therefore in agreement with the western blot analysis. Expression of HMGN1 was 1.7-fold lower, comparatively, in THP-1, and then decreased stepwise in K562, OCI-AML3 and MOLM-13, which displayed the lowest mRNA expression levels of HMGN1 at 374.5 nTPM. RNAseq analysis of these cell lines largely agreed with the western blot; except for MOLM-13 cells where HMGN1 protein was not detectable by western blot.

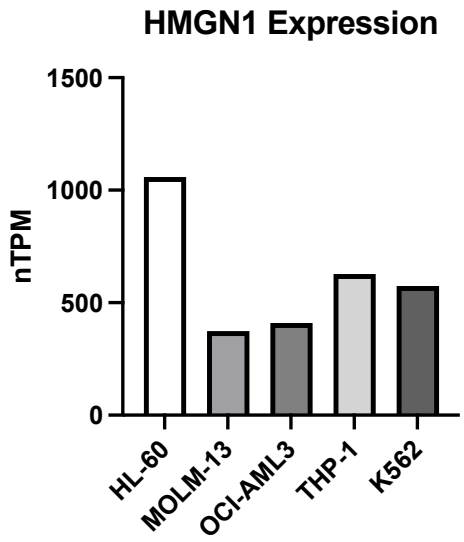

Figure 4. HMGN1 mRNA expression in a panel of myeloid leukaemia cell lines. RNAseq datasets from Protein Atlas [43] for the indicated cell lines were analysed; data shown is normalised Transcripts per million (nTPM).

3.2 Generation of HMGN1-Knockdown and -overexpression cell lines.

With the baseline expression levels of HMGN1 in the panel of myeloid leukaemia cell lines characterised, we then sought to determine the phenotypic effects of HMGN1 knock-down or over-expression in these cell lines.

Lentiviral transfection and transduction were performed to generate inducible shRNA-HMGN1 cell lines from the panel. First, HEK 293 LentiX cells were transfected with the lentiviral vector, packaging plasmids and desired RNA/DNA. Virus-containing media was collected from transfected HEK cells 48 hrs later and was applied to CML/AML cell lines to confer viral transduction.

The lentiviral vectors conferred puromycin resistance to successfully transduced cells. A concentration gradient of puromycin was therefore applied to each parental cell line within the panel to generate a kill curve and identify the optimum puromycin concentration for selection. An optimum puromycin concentration for selection was deemed the lowest concentration that will kill non-transduced cells. For each line, cells were seeded at a density of $1x10^5$ cells in a 6-well plate with 2ml of RPMI 10% FBS

media. Cells were treated with 6 puromycin concentrations ranging from 0 to 4 μg/mL. Cell viability was assessed at 0, 4, 8, 24 and 48hrs using Trypan blue staining and analysed on a Countess II Automated cell counter from ThermoFisher. A puromycin concentration that resulted in 10-20% viability after 48hrs for each cell line was deemed to be the most suitable for selection.

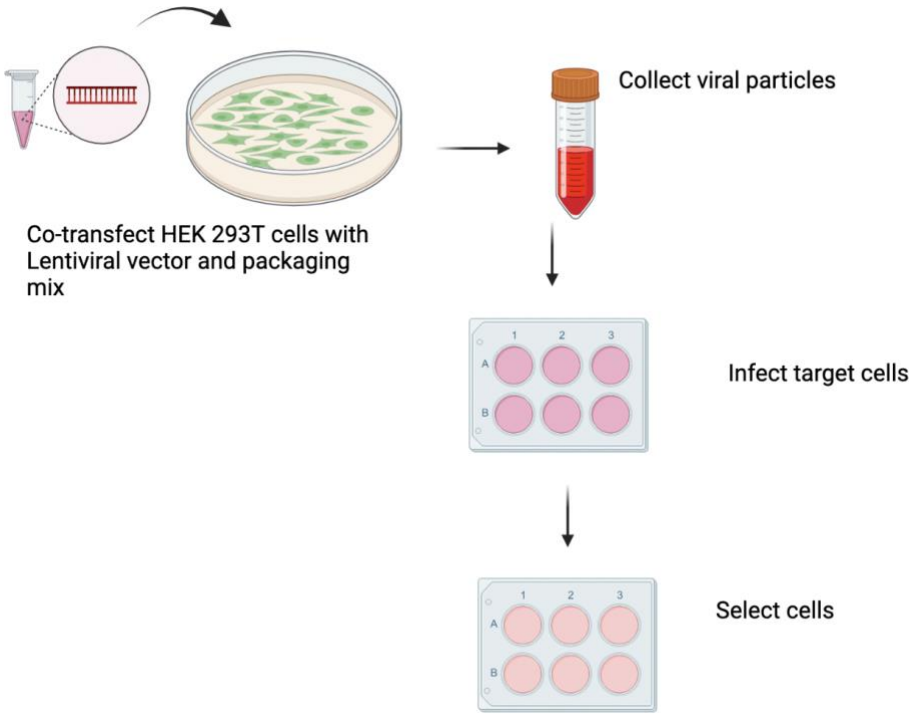

Figure 5. Schematic representation of viral transduction protocol. HEK 293 LentiX cells were transfected with psPAX2 (packaging plasmid), pMD2.G (envelope and lentiviral plasmid) and the desired coding sequence to either knockdown or overexpress to generate viral particles for transduction of AML cell lines. Cells were subsequently treated with puromycin to select virally transduced cells. Image generated using BioRender.

The optimum puromycin concentration for HL-60 was 1 μg/mL (Figure 6A), which was the lowest concentration that reduced viability below 20% after 48hrs (approx. 15% viability). For MOLM-13 cells, the optimal concentration was 0.5 μg/mL (Figure 6B), and although it gave a viability of 8% after 48hrs, all lower concentrations had a viability above 30% which would not have been suitable for cell selection. With THP-1 cells, the most suitable concentration was 0.50 μg/mL as it was the lowest concentration that would have viability within the suitable threshold (16% viability). Finally, for OCI-

AML3 cells, 0.5 μg/mL was the lowest concentration that reduced viability below 20% after 48hrs (approx. 19% viability).

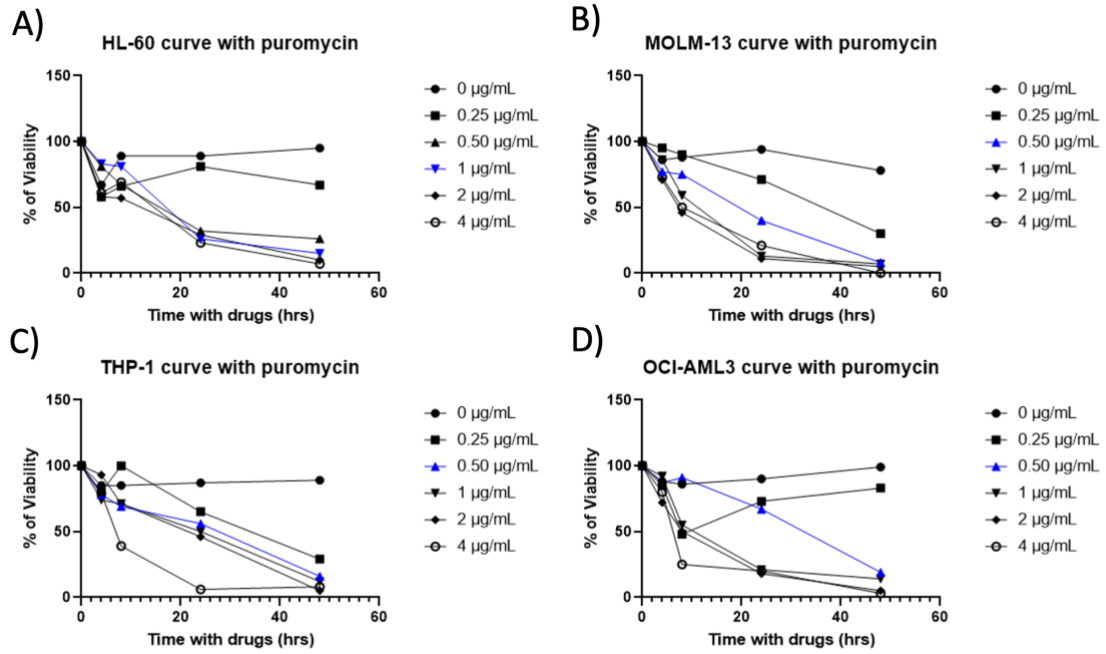

Figure 6. Determination of puromycin concentration for selection of virally transduced myeloid leukaemia cell lines. For each cell line, 1x10^5 cells per well were seeded in RPMI cell culture media with the indicated concentrations of puromycin. Cell viability was measured at 0, 4, 8, 24 and 48hrs using trypan blue and a Countess II Automated cell counter from ThermoFisher. The blue line in each graph represents the selected concentration. A) HL-60 cell line puromycin kill curve. n= 1. B) MOLM-13 cell line puromycin kill curve. n= 1. C) THP-1 cell line puromycin kill curve. n= 1. D) OCI-AML3 cell line puromycin kill curve. n= 1.

3.3 Determination of effective Doxycycline concentration to induce HMGN1 knockdown in virally transduced AML cell lines.

To generate inducible shRNA HMGN1 cell lines, shRNA sequences were generated that targeted two different regions within the HMGN1 mRNA sequence: coding sequence 1 (CDS1)-targeting and coding sequence 2 (CDS2)-targeting (Appendix 3). A non-targeting scrambled shRNA (Scr-shRNA) was used as a transduction control. The efficacy of HMGN1 knockdown by CDS1-shRNA and CDS2-shRNA was compared.

To generate an inducible-knockdown cell line, the doxycycline-inducible promoter pLKO-Tet-On plasmid was used. This system, as the name suggests, uses doxycycline to induce or “activate” the knockdown; when doxycycline is not present in the system, cells maintain endogenous HMGN1 protein levels. First, we determined the optimum concentration of doxycycline that induced an effective knockdown of HMGN1 with minimal cytotoxicity.

To assess optimal doxycycline concentration, transduced cell lines were treated for 72hrs with a concentration gradient of doxycycline: 0, 0.05, 0.5, 1, 2.5 and 5 μg/mL. At 72hrs post-treatment the cell viability was assessed. Protein levels of HMGN1 were assessed by western blot and quantified using ImageJ to ascertain knock-down efficiency.

In transduced HL-60 cells, 72hrs of the lowest concentration of doxycycline (0.05μg/mL) treatment resulted in 92% viability, 0.5μg/mL and 1μg/mL also maintained good viability (>90%) (Figure 7A). The highest concentrations (2.5μg/mL, 5μg/mL) of doxycycline reduced viability to 24%/ 65%, respectively, after 72hrs. Western blot and densitometric analysis of lysates from the aforementioned doxycycline concentration treatments demonstrated robust knockdown of HMGN1 protein between 0.05-5μg/mL (Figure 7B). Given that viability was unaffected by 0.05-1μg/mL doxycycline treatments, 0.05μg/mL was selected for induction as it demonstrated a 76% knock-down of HMGN1 expression compared to the uninduced HL-60 sample, whilst maintaining very good viability.

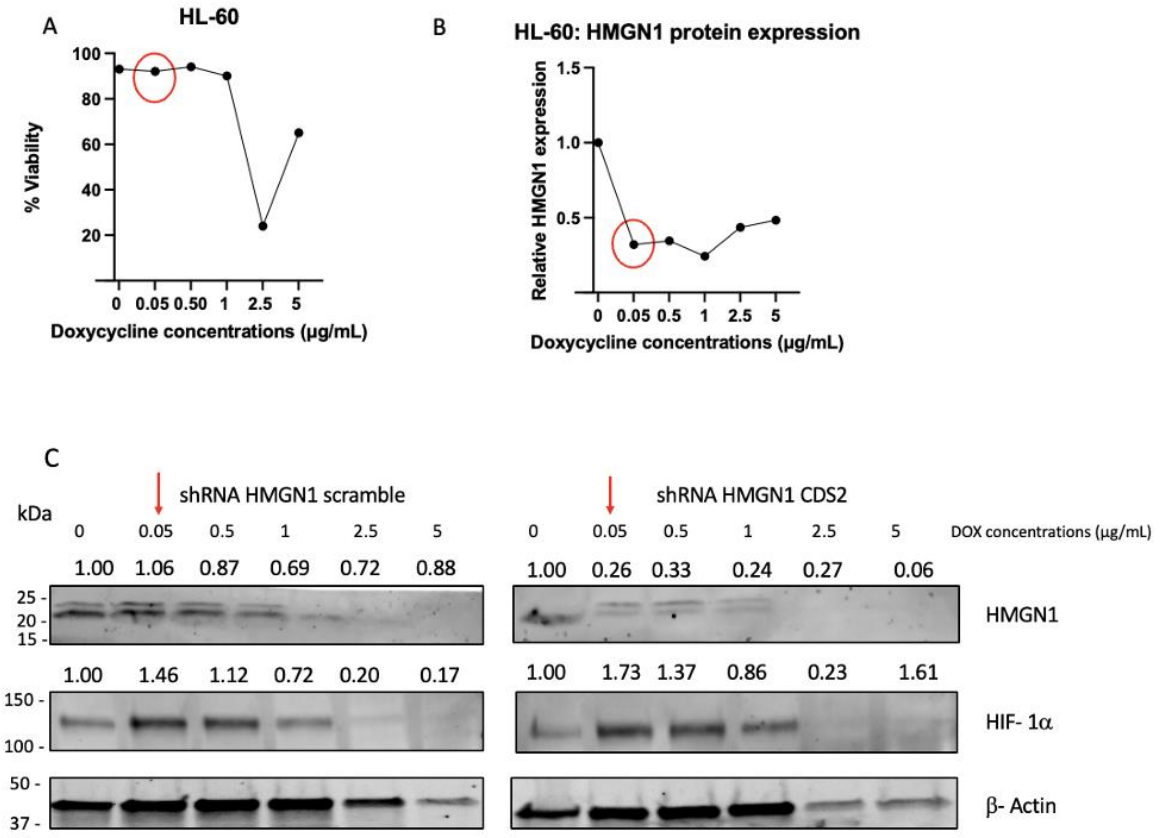

Figure 7. Cell viability and relative HMGN1 protein expression in HL-60 shRNA HMGN1 cell line after doxycycline induction. A) Percentage of viable cells after 72hrs doxycycline treatment at the indicated concentrations; viability was assessed using Trypan blue on a Countess. B) Densitometric analysis of HMGN1 protein levels in HL-60 cells transduced with shRNA HMGN1 CDS2 determined by western blot. Red circle indicated the selected doxycycline concentration which is the lowest concentration that maintains high cell viability whilst inducing effective HMGN1 protein knockdown. C) Western Blot analysis of HMGN1 protein levels in virally transduced HL-60 cells (either shRNA-Scrambled or shRNA HMGN1-CDS2), treated with the indicated concentration gradient of doxycycline for shRNA induction. HIF-1α protein levels were also determined, and β-Actin used as a loading control. Densitometric values displayed are of HMGN1 bands and normalised against β-Actin and 0μg/mL doxycycline. Red arrow indicates the concentration of doxycycline selected for induction in future experiments. Representative of n=4.

In transduced K562 cells, the lowest concentration range of doxycycline (0.05μg/mL - 1μg/mL) treatment resulted in approximately 96% viability (Figure 8A). The highest concentrations (2.5μg/mL, 5μg/mL) of doxycycline reduced viability to 62% and 75%,

respectively, after 72hrs. Western blot and densitometric analysis of lysates from the previously mentioned doxycycline concentration treatments demonstrated robust knockdown of HMGN1 protein between 0.05-5μg/mL (Figure 8B). Given that viability was unaffected by 0.05-1μg/mL doxycycline treatments, 0.05μg/mL was selected for induction as it demonstrated an approximate 50% knockdown of HMGN1 expression compared to the uninduced K562 sample (Figure 8), whilst maintaining very good viability.

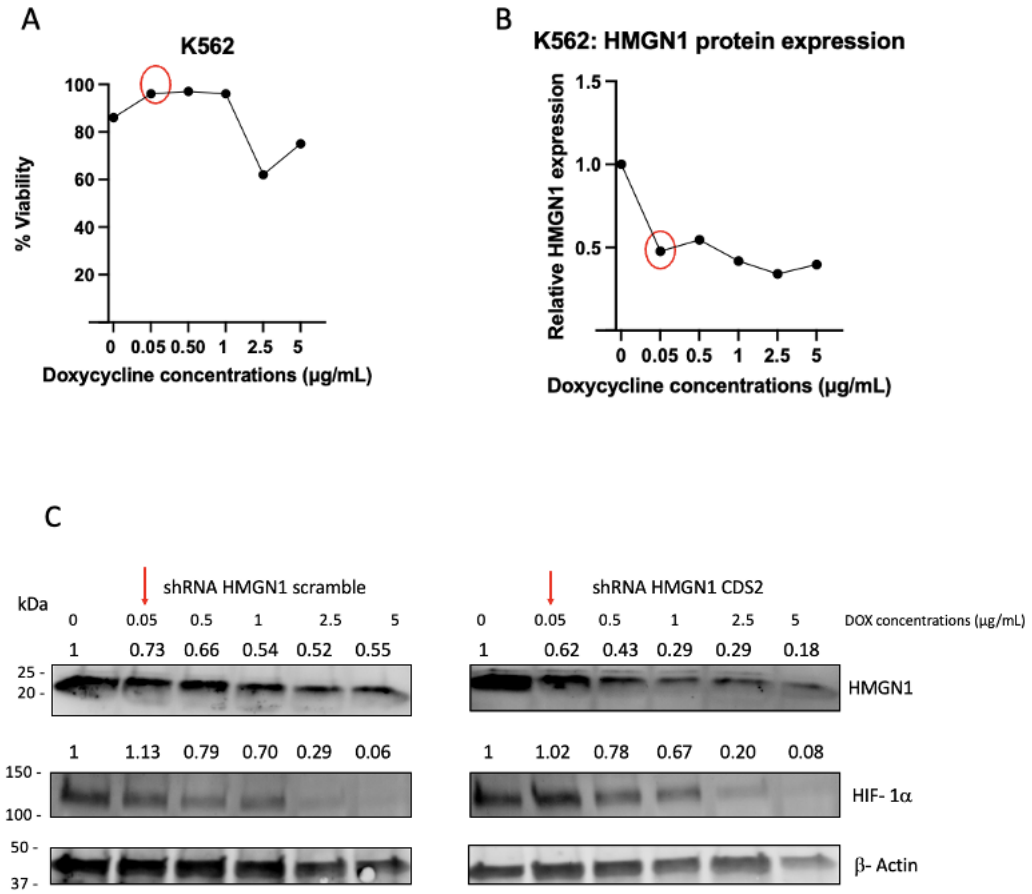

Figure 8. Cell viability and relative HMGN1 protein expression in K562 shRNA HMGN1 cell line after doxycycline induction. A) Percentage of viable cells after 72hrs doxycycline treatment at the indicated concentrations; viability was assessed using Trypan blue on a Countess. B) Densitometric analysis of HMGN1 protein levels in K562 cells transduced with shRNA HMGN1 CDS2 determined by western blot. Red circle indicated the selected doxycycline concentration which is the lowest concentration that maintains high cell viability whilst inducing effective HMGN1 protein knockdown. C) Western Blot analysis of HMGN1

protein levels in virally transduced K562 cells (either shRNA-Scrambled or shRNA HMGN1-CDS2), treated with the indicated concentration gradient of doxycycline for shRNA induction. HIF-1α protein levels were also determined, and β-Actin used as a loading control. Densitometric values displayed are of HMGN1 bands and normalised against β-Actin and 0μg/mL doxycycline. Red arrow indicates the concentration of doxycycline selected for induction in future experiments. Representative of n=3.

3.4 Validation of shRNA HMGN1 cell lines

After selecting the optimal doxycycline concentration for K562 and HL-60 transduced cell lines, we next determined whether the CDS1-targeting or CDS2-Targeting shRNAs conferred better knockdown in each cell line. Cells were treated with 0.05 μg/mL doxycycline for 72hrs; cells that were treated with hypoxia were incubated in a hypoxic chamber at 1% O_2 for the final 4 hrs of treatment.

K562 cells were transduced with shRNA HMGN1 scrambled (Scr), shRNA HMGN1 CDS1 and shRNA HMGN1 CDS2 and then assessed by western blot to determine relative HMGN1 expression and degree of knockdown. Comparison of K562 shRNA CDS1 and CDS2 samples under both hypoxia and normoxia demonstrated that CDS1 conferred sufficient HMGN1 knockdown (approximately 30%), whereas CDS2 seemingly increased HMGN1 protein levels instead of the expected knockdown. For this reason, CDS1 was selected as the optimal shRNA to knock down HMGN1 in K562 cells.

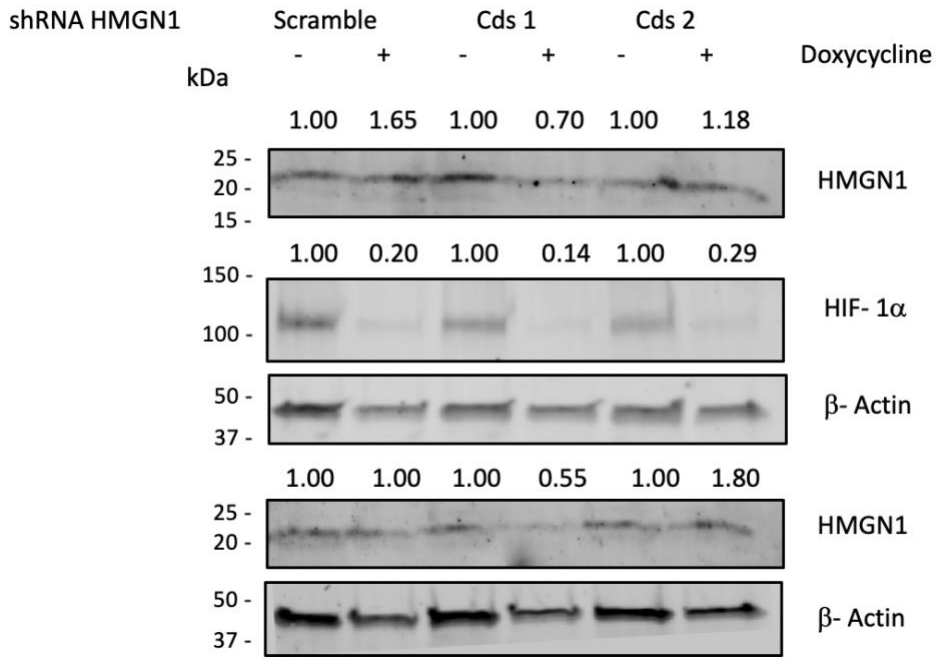

Figure 9. Protein levels in the transduced shRNA HMGN1 K562 cells. Western blot analysis of HMGN1 in the indicated transduced cell lines with shRNA HMGN1 cultured under normoxic conditions (20% O_2) or hypoxic conditions (1% O_2, 4 hours). HIF-1α levels and quantification performed on hypoxic samples. β-Actin loading control. Densitometric values displayed are of HMGN1 bands normalised against β-Actin and untreated doxycycline samples. Representative of n=4.

For the HL-60 cell line, both shRNA CDS1 and CDS2 conferred demonstrable knockdown of HMGN1 in hypoxia and normoxia, with CDS1 demonstrating a slightly more efficient knockdown (Figure 10). We did observe, however, that HIF-1α protein levels in hypoxic samples were seemingly affected in CDS1, therefore CDS2 was chosen for further experiments as it gave a relatively good knockdown and showed kept similar HIF-1α levels to its control.

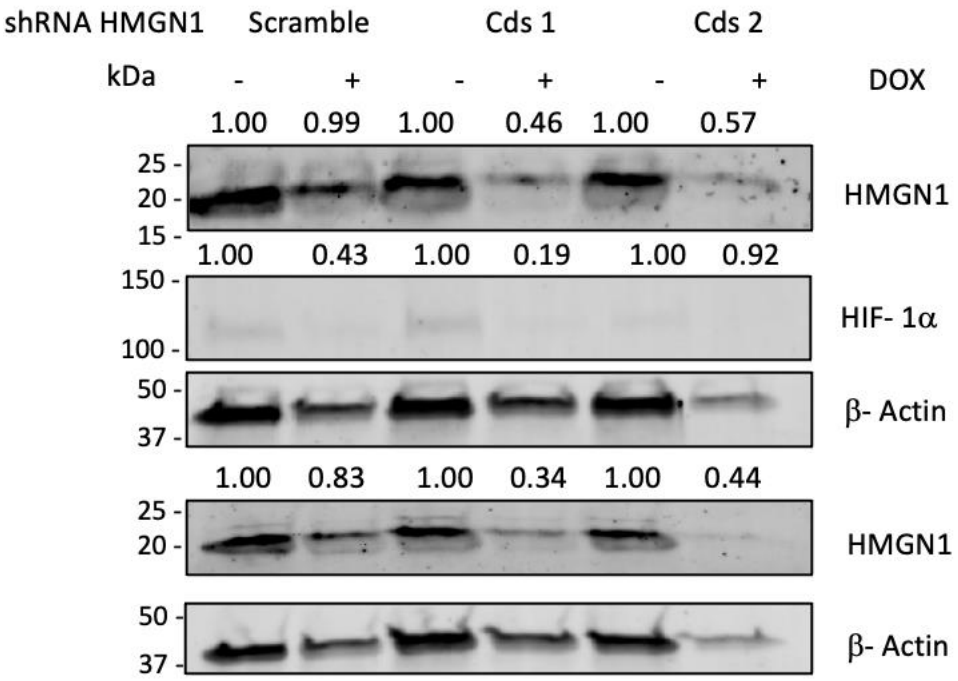

Figure 10. Protein levels in the transduced shRNA HMGN1 HL-60 cells. Western blot analysis of HMGN1 in the indicated transduced cell lines with shRNA HMGN1 cultured under normoxic conditions (20% O_2) or hypoxic conditions (1% O_2, 4 hours). HIF-1α levels and quantification performed on hypoxic samples. β-Actin loading control. Densitometric values displayed are of HMGN1 bands normalised against β-Actin and untreated doxycycline samples. Representative of n=3.

For the MOLM-13 cell line, both shRNA CDS1 and CDS2 conferred demonstrable knockdown of HMGN1 in hypoxia and normoxia, with CDS1 demonstrating a more efficient knockdown (Figure 11). We did observe that in hypoxia the knockdown was more significant compared to normoxia. As shRNA CDS1 showed a better knockdown overall CDS1 was chosen for further experiments.

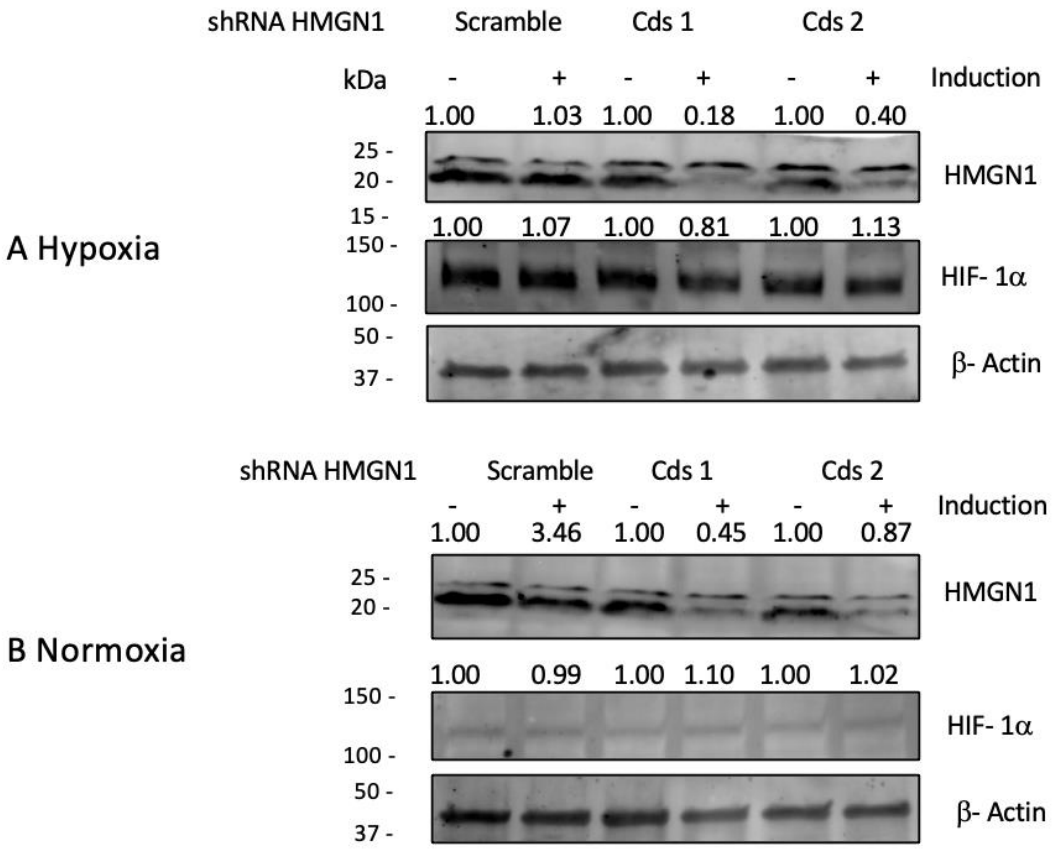

Figure 11. HMGN1 protein levels in the transduced HMGN1 MOLM-13 cells. Western blot analysis of HMGN1 in the indicated transduced cell lines with shRNA HMGN1 cultured under normoxic conditions (20% O_2) or hypoxic conditions (1% O_2, 4 hours). HIF-1α levels and quantification performed, β-Actin loading control. Densitometric values displayed are of HMGN1 bands normalised against β-Actin and untreated doxycycline samples. Representative of n=3.

For the OCI-AML3 cell line, the cells were transduced with shRNA HMGN1 scramble, shRNA HMGN1 CDS1 and shRNA HMGN1 CDS2. However, only the shRNA HMGN1 CDS1 was successful for OCI-AML3 as it was the only one that was effectively selected with puromycin. The western blot showed that in normoxic conditions the knockdown was only about 25% compared to the uninduced cells and in hypoxic conditions, there wasn't a good knockdown to see (Figure 12).

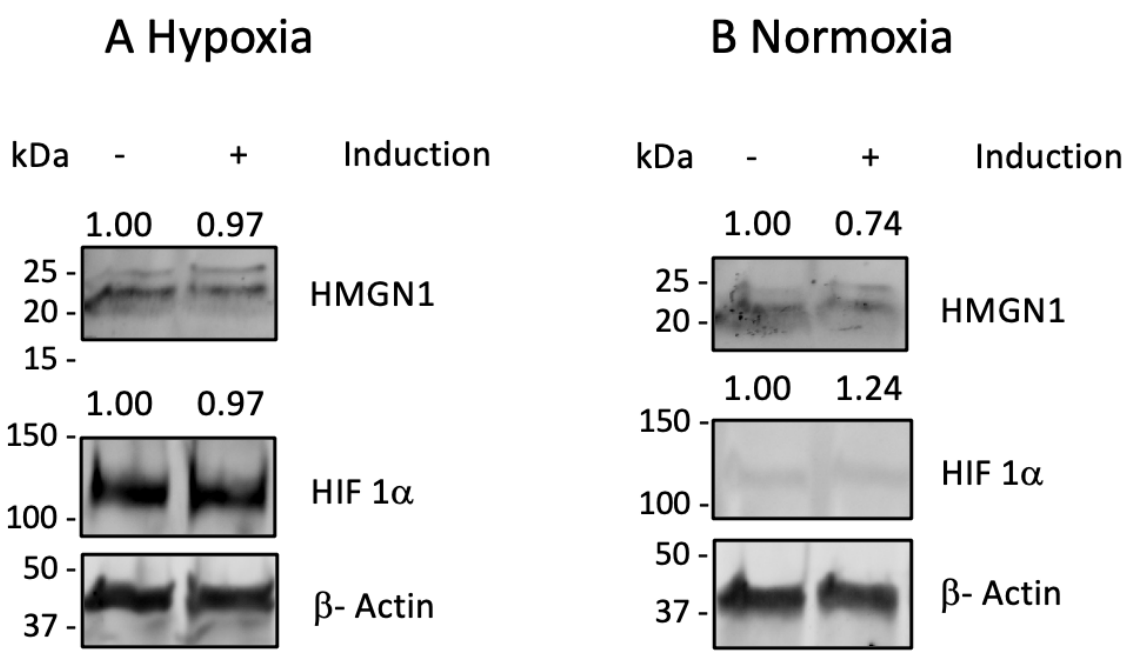

Figure 12. Protein levels in the transduced shRNA HMGN1 OCI-AML3 cells. Western blot analysis of HMGN1 in the indicated transduced cell lines with shRNA HMGN1 cultured under normoxic conditions (20% O_2) or hypoxic conditions (1% O_2, 4 hours). HIF-1α levels and quantification performed, β-Actin loading control. Densitometric values displayed are of HMGN1 bands normalised against β-Actin and untreated doxycycline samples. Representative of n=2.

3.5 Validation of the Overexpression system

HMGN1 overexpression cell lines were generated using the SBI SparQ Cumate Switch System. This system works by a CymR within the promoter, inducing supraphysiological expression (2-3 fold) of HMGN1 cDNA in the cell.

Induced cells were treated with cumate at a final concentration of 30μg/mL, as per the manufacturer's suggestion. HL-60 overexpression-induced cells treated with either normoxia or hypoxia demonstrated an increase in the HMGN1 protein expression (2.3 and 2.8-fold respectively).

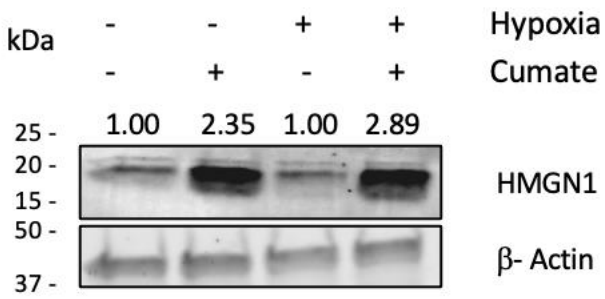

Figure 13. Protein levels in transduced HMGN1 overexpression HL-60 cells. Western blot analysis of HMGN1 in the indicated transduced cell lines with HMGN1 overexpression cumate system, cultured under normoxic conditions (20% O_2) or hypoxic conditions (1% O_2, 4 hours) n=1. β -Actin loading control. Densitometric values displayed are of HMGN1 bands normalised against β-Actin and untreated cumate samples.

MOLM-13 cells transduced with the overexpression vector and treated with cumate (as above) demonstrated an increase of 1.77-fold of HMGN1 protein expression compared to control under normoxia. However, under hypoxic conditions, cumate treatment did not visibly enhance HMGN1 protein levels (Figure 14).

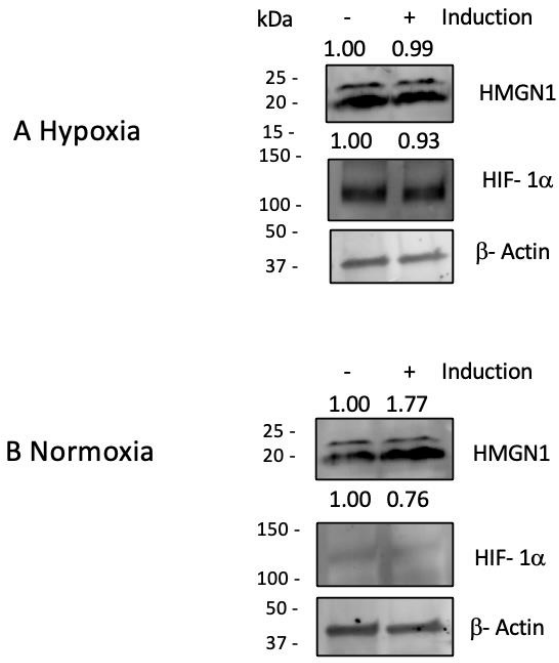

Figure 14. Protein levels in transduced HMGN1 overexpression MOLM-13 cells. Western blot analysis of HMGN1 in the indicated transduced cell lines with HMGN1 overexpression cumate system, cultured under normoxic conditions (20% O_2) or hypoxic conditions (1% O_2,

4 hours). HIF-1α levels and quantification performed, β-Actin loading control. Densitometric values displayed are of HMGN1 bands normalised against β-Actin and untreated cumate samples. Representative of n=3.

THP-1 cells transduced with the overexpression vector and treated with cumate demonstrated an increase of 1.50-fold of HMGN1 protein expression compared to control under normoxia; however, under hypoxic conditions, cumate treatment did not visibly enhance HMGN1 protein levels (Figure 15).

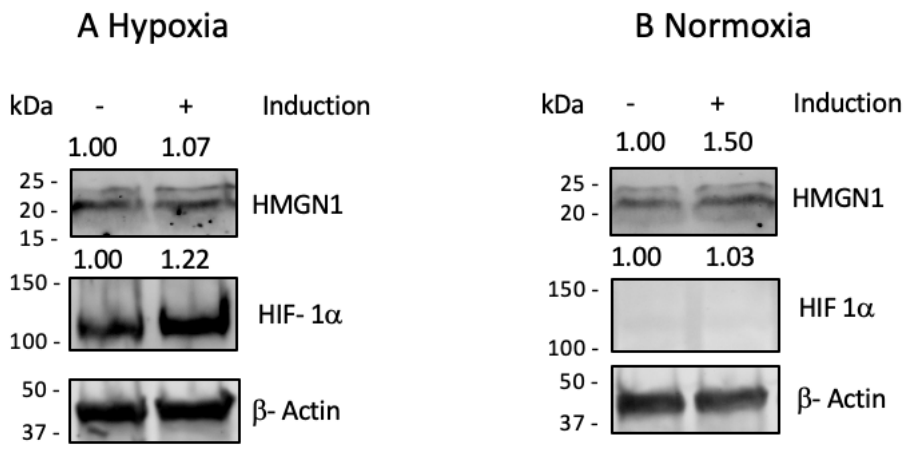

Figure 15. Protein levels in transduced HMGN1 overexpression THP-1 cells. Western blot analysis of HMGN1 in the indicated transduced cell lines with HMGN1 overexpression cumate system, cultured under normoxic conditions (20% O_2) or hypoxic conditions (1% O_2, 4 hours). HIF-1α levels and quantification performed, β-Actin loading control. Densitometric values displayed are of HMGN1 bands normalised against β-Actin and untreated cumate samples. Representative of n=2.

3.6 Assessing the effect of HMGN1 in HIF target genes

To assess the effect of knocking down or overexpressing HMGN1 upon HIF-1 transcription activity, first a hypoxia time course was performed and the relative levels of 2 canonical HIF-1 target genes (VEGFA and VLDLR) were analysed by RT-qPCR. The purpose of the hypoxia time course was to determine the optimum conditions to

analyse the induction of these HIF-1 target genes and whether HMGN1 knockdown/ overexpression regulated HIF-1 transcription activity.

A RT^2 Profiler PCR Array Human Hypoxia Signalling Pathway Plus (QIAGEN, PAHS-032YA) was performed in the Bridge Laboratory by Dr David Kealy. The assay allowed to choose the top differentially expressed genes from the profile (total of 89 genes screened). Although, this was performed with the original reporter cell line A549, a lung adenocarcinoma, as this was the cell line that Dr Katherine Bridge conducted the initial CRISPR screen where HMGN1 was identified as a positive regulator of HIF. The same top hits genes were chosen for this project as they were the top hits with the HMGN1 knockdown cell line.

Hypoxic incubations were conducted for 0hrs, 4hrs, 16hrs, 24hrs and 48hrs at 1% O_2 within the 72-hour HMGN1 knockdown/ overexpression induction window. The data gathered showed that although an effect could start to be seen at 4hrs of hypoxic induction at 48hrs the effect seen is greater and significant for both induced and non-induced cells compared to normoxic conditions. Also, it was considered that this time point (48 hrs) recaptures more faithfully the mechanism of hypoxia that occurs in patients.

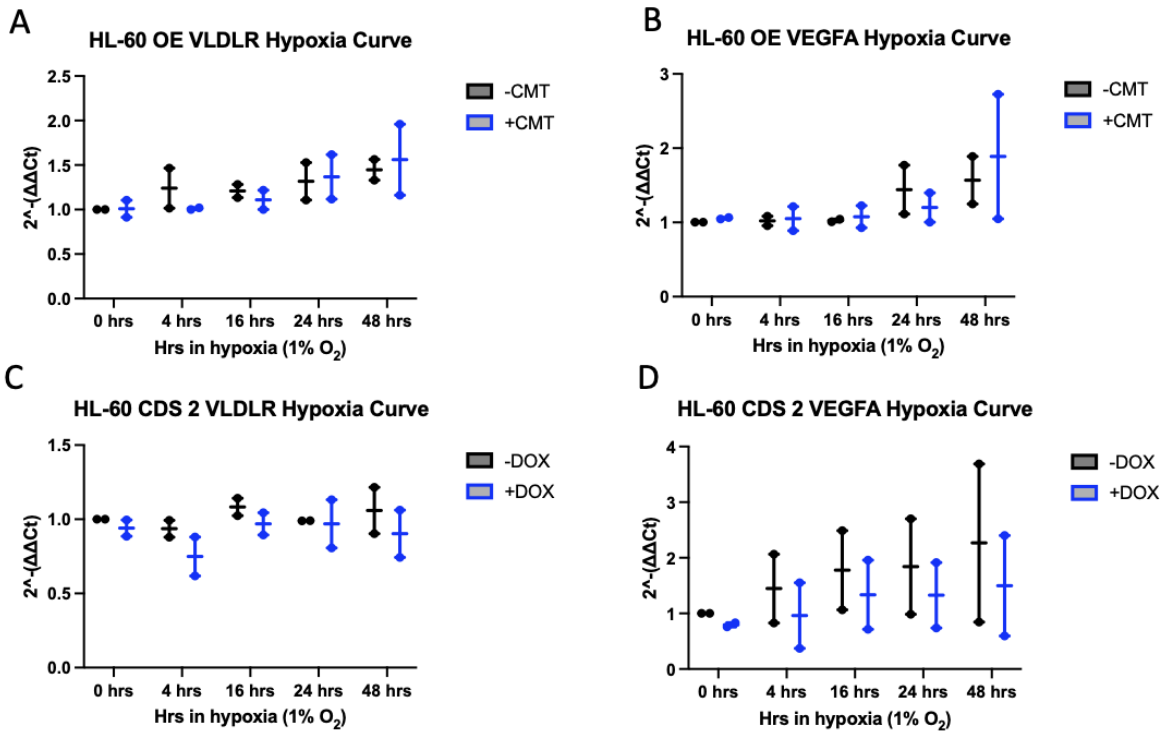

Figure 16. Hypoxia curves assessed by RT-qPCR for analysis of the effect of HMGN1 in HIF target genes. RT-qPCR of HL-60 shRNA HMGN1 CDS2 and HMGN1 Overexpression cell lines. The time points that were analysed were: 0hrs (normoxia), 4hrs, 16hrs, 24hrs and 48hrs in the cell culture at 1% O_2 previously to RNA extraction but overall, in culture for 72hrs with the inducible reagent (doxycycline or cumate). n=2.

The next step to assess the effect of HMGN1 in the HIF target genes was to run RT-qPCR with a panel of HIF-1 target genes, including VLDLR, VEGFA, MIF, LDHA, GLUT1, CDKN1A and CA9. Also, HMGN1 and HIF-1α mRNA expression levels were evaluated to confirm as they would assess the knockdown/ overexpression inductions and any off-target effects on HIF-1α expression.

HIF-1α mRNA levels are not expected to change under different oxygen conditions as HIF-1α is constitutively expressed and the protein is degraded under normoxic conditions.

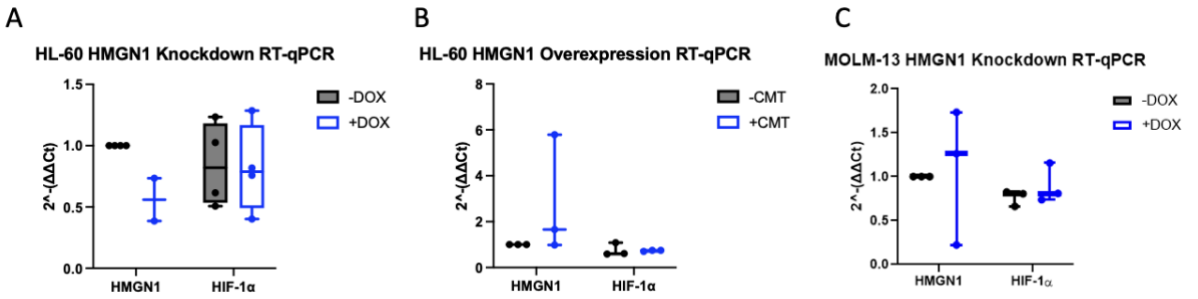

Figure 17. RT-qPCR for HMGN1 and HIF-1α as validation of the samples. RT-qPCR of HL-60 shRNA HMGN1 CDS2 and HMGN1 overexpression cell lines evaluating HMGN1 and HIF-1α RNA expression. Samples were incubated in hypoxia (1% O_2) for 48hrs. n=3.

The RT-qPCR results of the different target genes showed that knocking down HMGN1 in HL-60 would result in no statistically significant change in VLDLR, MIF, LDHA, GLUT1 and CA9 HIF target genes. However, a couple of genes can be observed that were affected by knocking down the expression of HMGN1. Both VEGFA and CDKN1A were downregulated when HMGN1 expression was also knockdown as observed in Figure 18A.

Furthermore, knocking down HMGN1 expression in the MOLM-13 cell line showed one gene had been affected by it. With this cell line, VLDLR was upregulated whilst the other genes did not have a statistically significant change as can be seen in Figure 18B.

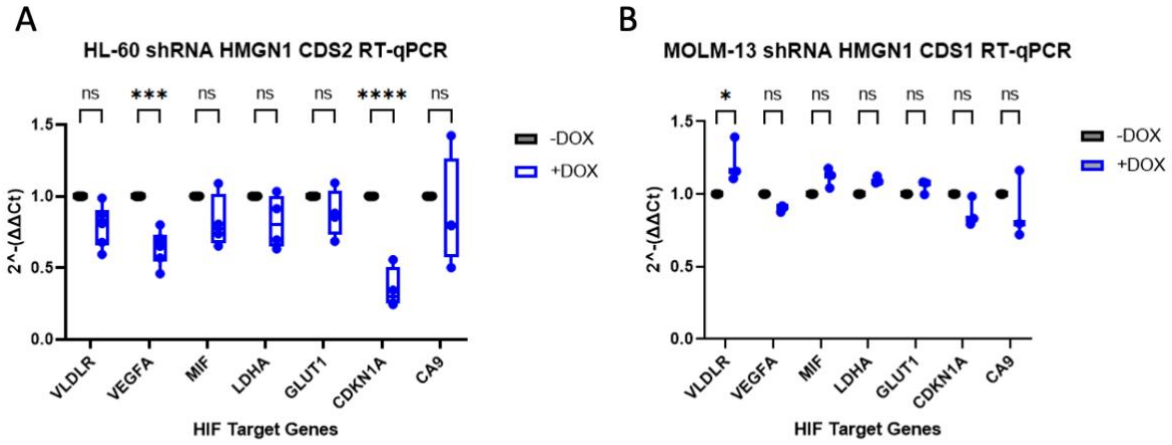

Figure 18. RT-qPCR results of HIF Target genes in HL-60 and MOLM-13 cell lines with HMGN1 knockdown in hypoxic conditions (1% O_2). Samples were analysed after they were

treated in hypoxia for 48hrs and induced knockdown with doxycycline for 72hrs. To compare the data a two-way ANOVA test was used. A) shows HL-60 cell line analysis of the regulation of 7 different HIF target genes. Where VEGFA showed a statistically significant down-regulation with a p-value of 0.0003 and CDKN1A also showed a statistically significant down-regulation with a p-value of <0.001. The other genes did not show any statistical difference in either up- or down-regulation in Hypoxia when HMGN1 was knocked down. n= 4, and for VLDLR and VEGFA n= 6. B) shows MOLM-13 cell line analysis of the regulation of 7 different HIF target genes. Where VLDLR showed a statistically significant up-regulation with a p-value of 0.0231. n= 3.

RT-qPCR data results for the HL-60 HMGN1 overexpression cells did show that none of the genes tested were significantly altered in their expression levels when HMGN1 was overexpressed (Figure 19).

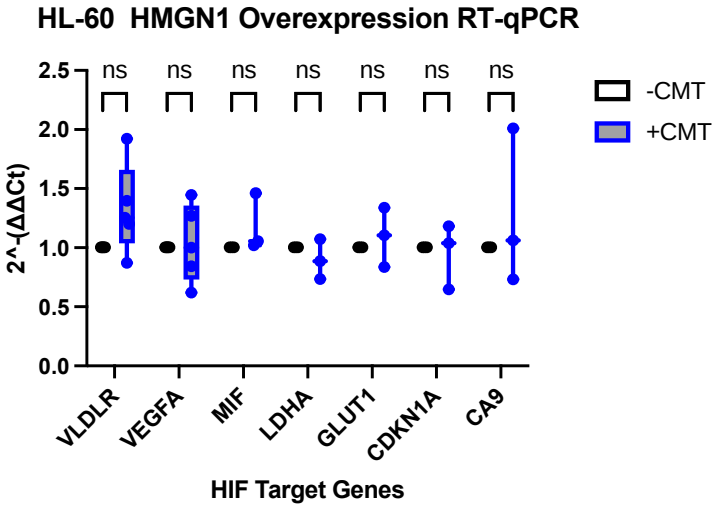

Figure 19. RT-qPCR results of HIF Target genes in HL-60 cell line with HMGN1 overexpression in hypoxic conditions (1% O_2). Samples were analysed after they were treated in hypoxia for 48hrs and induced overexpression with Cumate for 72hrs. To compare the data a two-way ANOVA test was used. The graph shows that none of the genes suffered a statistically significant up- or down-regulation; however, the overexpression induction was not working when cells are with cumate in the hypoxia incubator (1% O_2). n= 3, and for VLDLR and VEGFA n= 5.

We, therefore, analysed these cells by western blot; conversely, after looking at all the data together and the western blot in Figure 20 we can infer that this specific result is due to no HMGN1 overexpression induction from cumate at 1% O_2. In Figure 17B, the expression of HMGN1 is not induced in all samples successfully. Additionally, some of the reactions gave uncertainty when assessing HMGN1 due to a problem with the HMGN1 primers. The protein samples were assessed with western blots for both HMGN1 and HIF-1α. The hypoxic samples were successfully induced as HIF-1α protein can be observed on the samples. Furthermore, with HMGN1 a relatively good knockdown can be seen on the shRNA HMGN1 CDS2 samples. However, for the overexpression samples, the overexpression of HMGN1 was only successfully achieved in the normoxic samples.

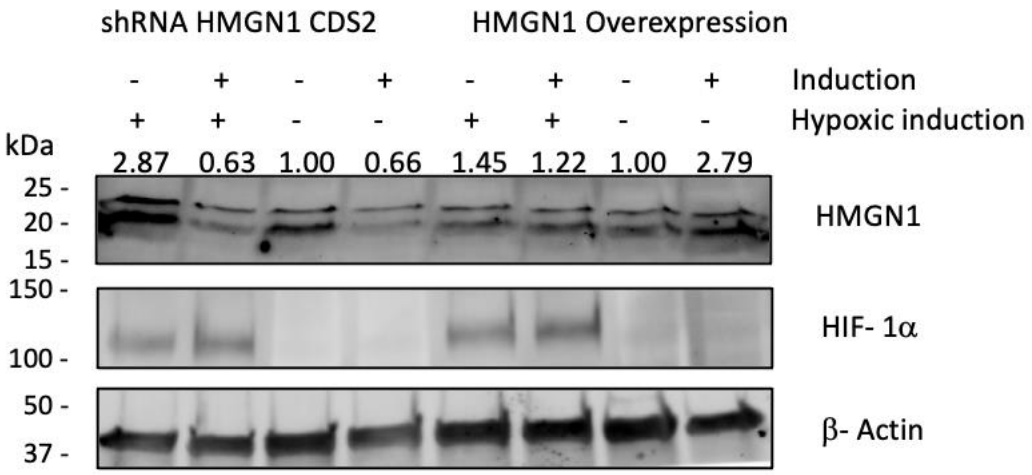

Figure 20. Protein levels of HMGN1 and HIF-1α. Western blot of HMGN1 and HIF-1α protein expression after 72hrs of either doxycycline (shRNA HMGN1 CDS2) or cumate (HMGN1 overexpression) and 48hrs of hypoxia induction (1% O_2), Samples with no induction were treated the same without adding the drugs and if needed were kept in the normoxic incubator (20% O_2). β-Actin loading control. Densitometric values displayed are of HMGN1 bands normalised against β-Actin. HIF-1α was not quantified as it was just to observe if hypoxic induction occurred or not in the samples. Representative of n=2.

3.7 Assessing the effect of HMGN1 and HIF-1α in the Colony Formation Unit Assay

To assess more characteristics of the impact of HMGN1 and HIF-1α in AML cell lines the Colony Formation Unit (CFU) assay, which would analyse the cell line capacity to proliferate and differentiate was performed. This assay was prepared using the HIF-1α inhibitor GN44028. This inhibitor is a HIF-1α-specific inhibitor focused on inhibiting the transcriptional activity of HIF-1 without affecting the levels of HIF-1α in the cells [44]. This drug does not affect the heterodimerization of HIF-1α and HIF-1β in the nucleus of the cells [44].

Firstly, HL-60 shRNA HMGN1 CDS2 and HL-60 HMGN1 Overexpression cells were assessed in normoxic conditions (20% O_2) considering that the overexpression cells were not induced if they were treated at 1% O_2. As for this set of assays would be ideal to have the pair on the same conditions.

The CFU assay showed that the first replicate for HL-60 shRNA HMGN1 CDS2 had a statistical significance on the colony count between the HMGN1 knockdown samples when compared to with and without the inhibitor with a p-value of 0.0035. The second replicate gave no statistical significance between conditions. The third replicate showed significance in the colony count between samples without induction but with and without the inhibitor (-DOX samples). Additionally, this replicate also showed a significant difference between the samples of no inhibitor (-GN44028) hence just comparing the HMGN1 knockdown. For this replicate the significant p-values in both cases were <0.0001. Furthermore, in Figure 21D, the trend of the mean colony count per biological replicate can be observed. Moreover, in Figure 22 the progression of the growth and formation of the colonies of the HL-60 shRNA HMGN1 CDS2 in different conditions can be observed. The images were taken using STEMvision on day 0, day 2, day 4, day 7 and day 10.

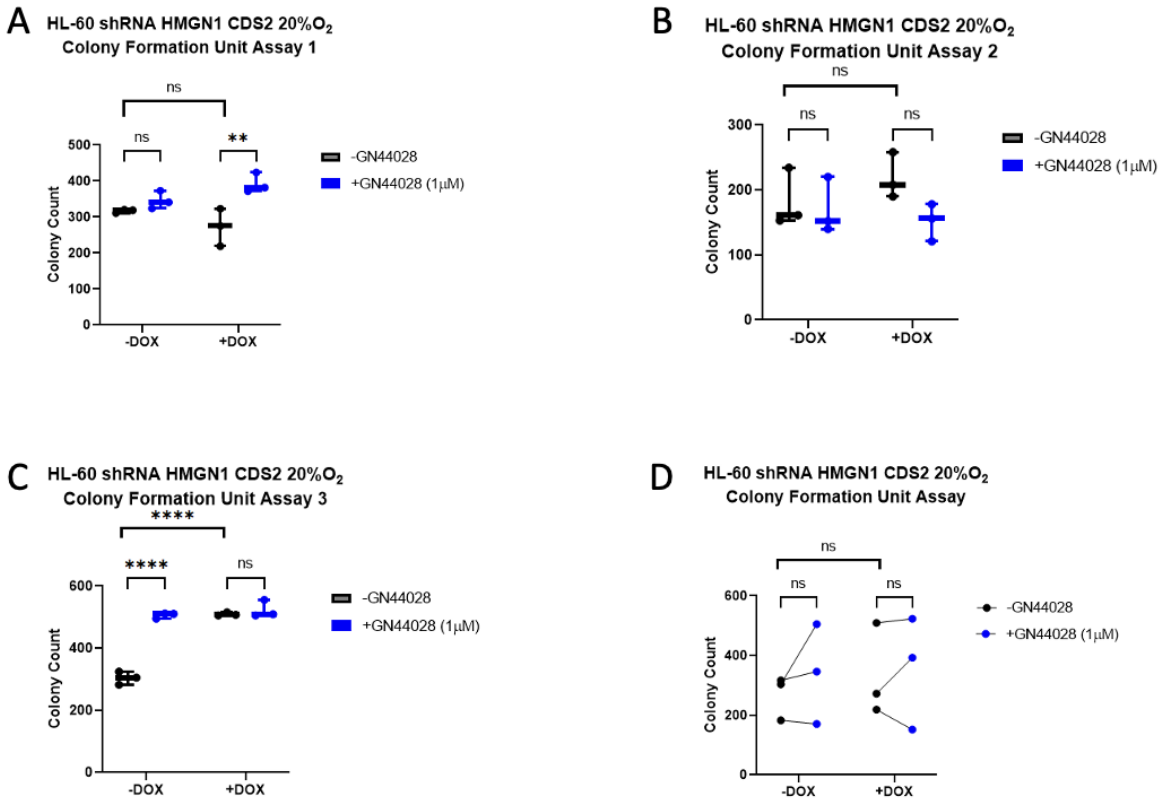

Figure 21. Colony Formation Unit assay in HL-60 shRNA HMGN1 CDS2 cell line. After 72hrs induction cells were seeded in their respective conditions in MethoCult at 20% with 3 technical replicates. The plates were scanned using STEMvision and images were analysed for colony count with Image J. To compare the data a two-way ANOVA test was used. n= 3. A) the first biological replicate each point represents a technical replicate. B) second biological replicate. C) third biological replicate. D) Plot of the mean of each technical replicate, each dot represents a biological replicate, and the lines are to observe the trend of each experiment.

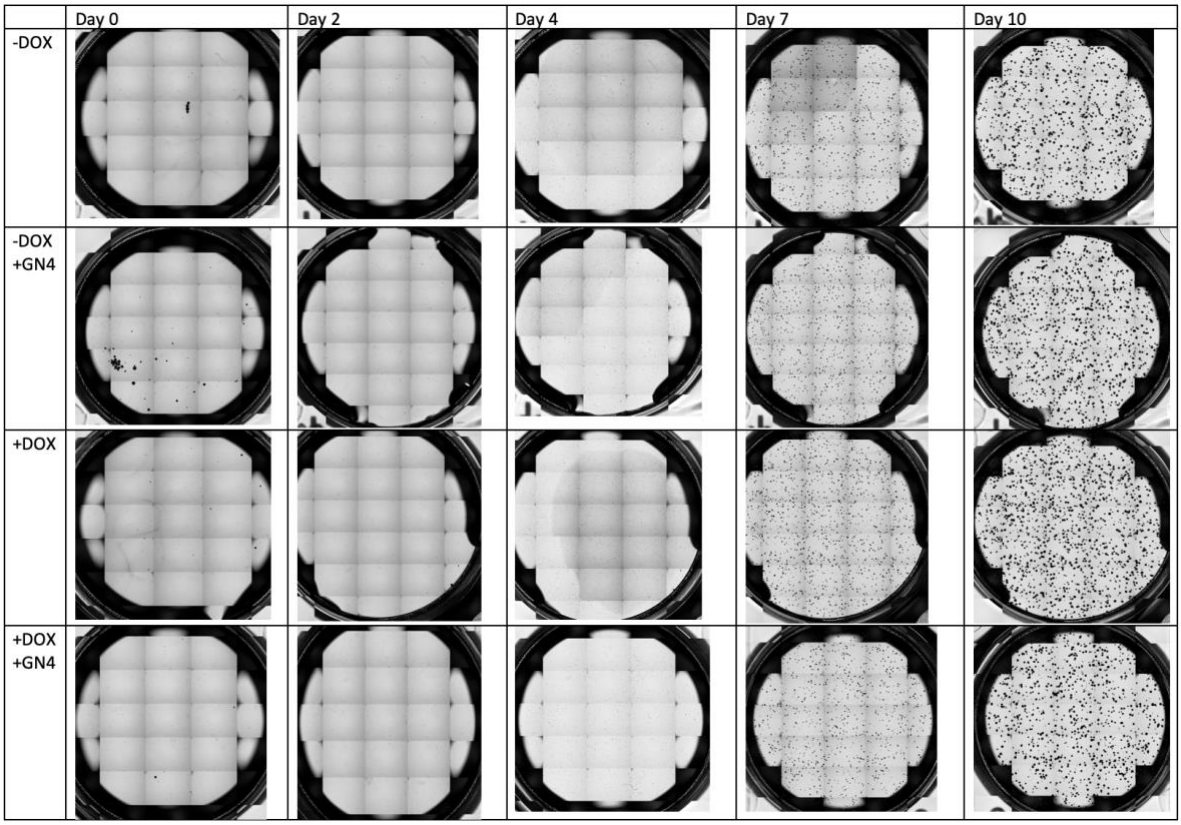

Figure 22. Representative well showing the colony formation of HL-60 shRNA HMGN1 CDS2 cells. Images were taken using STEMvision on day 0, day, 2, day 4, day 7 and Day 10. The four conditions used can be observed: the control (-DOX) which represents no induction and no HIF-1α inhibitor, -DOX +GN4 represents the well with no HMGN1 knockdown induction but does have 1μM final concentration of the HIF-1α inhibitor GN44028. +DOX represents HMGN1 knockdown induction but no HIF-1α inhibitor. And the last condition (+DOX +GN4) does have the HMGN1 knockdown induction and the HIF-1α inhibitor GN44028. Representative of a well of 1 replicate, n=3.

Paired with the Knockdown, the HL-60 HMGN1 overexpression CFU assay was also performed. The first replicate showed a statistical significance between non-induced samples where the p-value was 0.003 showing a significant increase in the number of colonies when the cells received 1μM of GN44028 HIF-1α inhibitor. Between the samples that were overexpressed, inhibiting HIF-1α caused a significant increase in the number of colonies with a p-value of <0.0001. Furthermore, the number of colonies between no overexpression and overexpressed HMGN1 cells showed a significant reduction of colonies when HMGN1 was overexpressed with a p-value of <0.0001.

The second replicate gave no statistical significance between the conditions when compared towards the HIF-1α inhibitor; however, it did show a significant change in the number of colonies between no overexpression induction and the induced sample with a p-value of 0.0024. The third replicate again showed a statistical significance between all conditions where the no induced overexpression cells with the presence of the HIF-1α inhibitor, the number of colonies increased (p-value 0.0185). The overexpressing HMGN1 samples also had a significant change; however, for these samples, the colony number was reduced with the presence of the HIF-1α inhibitor. Additionally, comparing the samples regarding HMGN1 induction, the cells overexpressing HMGN1 had an increased number of colonies compared to the no HMGN1 overexpression (p-value <0.0001).

Furthermore, in Figure 23D, the trend of the mean colony count per biological replicate can be observed, where the no induced samples all showed the same trend between replicates whilst the HMGN1 overexpress samples did not follow a trend. Moreover, in Figure 24 the progression of the growth and formation of the colonies of the HL-60 shRNA HMGN1 overexpression in different conditions can be observed.

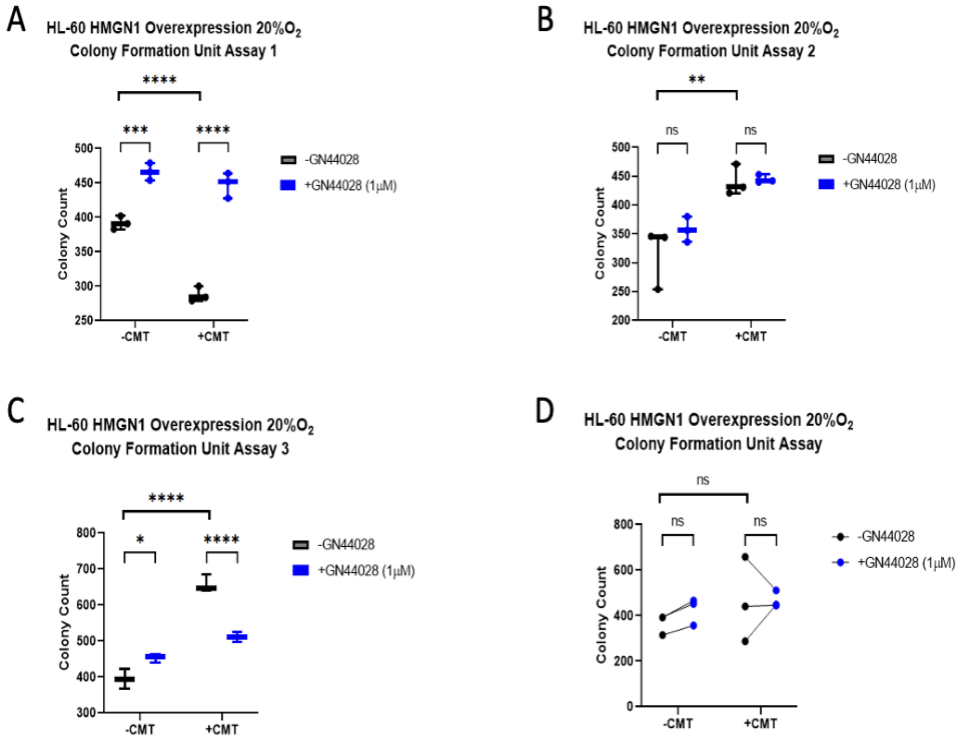

Figure 23. Colony Formation Unit assay in HL-60 HMGN1 overexpression cell line. After 72hrs induction cells were seeded in their respective conditions in MethoCult at 20% with 3 technical replicates. The plates were scanned using STEMVision and images were analysed

for colony count with Image J. To compare the data a two-way ANOVA test was used. n= 3. A) first biological replicate where each point represents a technical replicate. B) second biological replicate. C) third biological replicate. D) Plot of the mean of each technical replicate, each dot represents a biological replicate, and the lines are to observe the trend of each experiment.

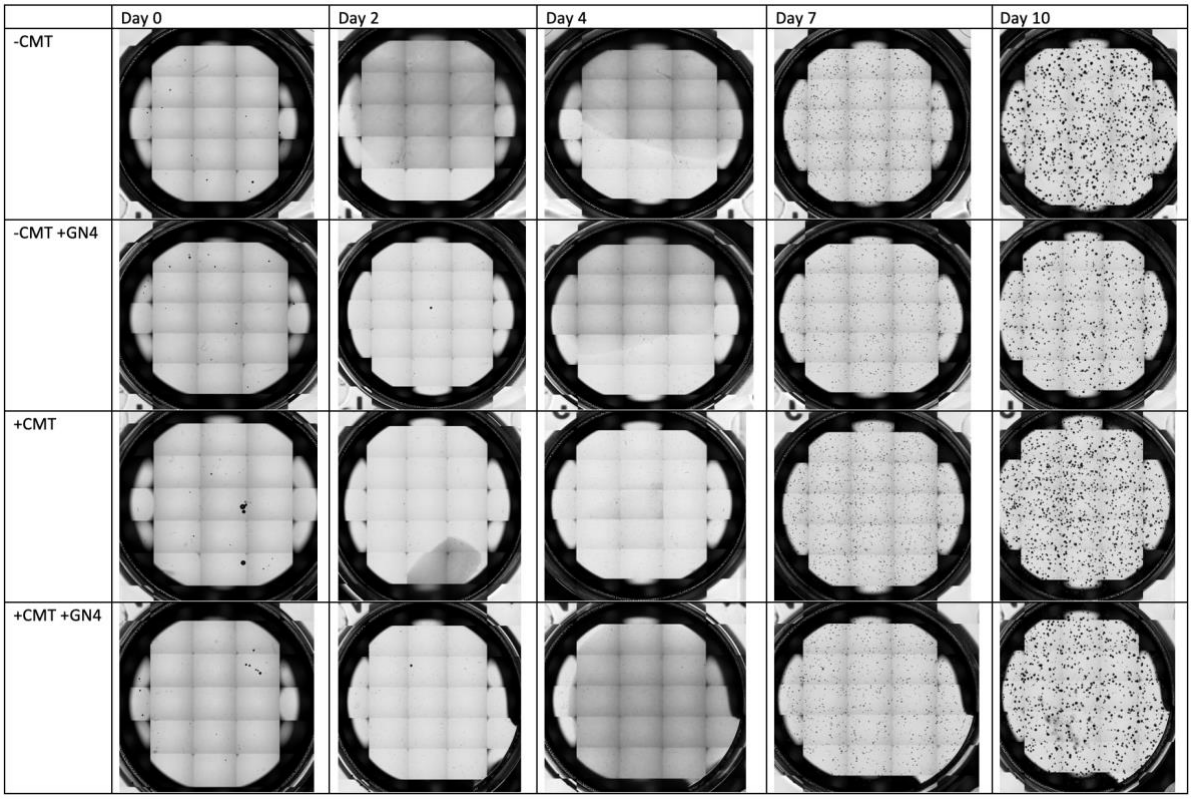

Figure 24. Representative well showing the colony formation of HL-60 HMGN1 overexpression cells. Images were taken using STEMvision on day 0, day 2, day 4, day 7 and Day 10. The four conditions used can be observed: the control (-CMT) which represents no induction and no HIF-1α inhibitor, -CMT +GN4 represents the well with no HMGN1 overexpression induction but does have 1μM final concentration of the HIF-1α inhibitor GN44028. +CMT represents HMGN1 overexpression induction but no HIF-1α inhibitor. And the last condition(+CMT +GN4) does have the HMGN1 overexpression induction and the HIF-1α inhibitor GN44028. Representative of a well of 1 replicate, n=3.

Another cell line that the CFU was performed with was MOLM-13 shRNA HMGN1 CDS1, contrary to the HL-60s this cell line was performed in hypoxic conditions (1% O_2). The first replicate showed no statistical significance of the change in the number

of colonies formed in any condition. However, after looking at the reduction in colony number in the induced cells with the HIF-α inhibitor when compared to the knockdown and no inhibitor the p-value was 0.0552, making it just by a margin not significant. The second replicate gave a statistical significance between the no induced samples with a p-value of 0.0168 where there was a reduction in the number of colonies for the cells with the HIF-α inhibitor. Additionally, the induced samples had a p-value of 0.0931. The third replicate showed no significance in the colony count between any of the samples. Moreover, in Figure 25D, the trend of the mean colony count per biological replicate can be observed, where all biological replicates followed the same trend. Also, in Figure 26 can be observed the progression of the growth and formation of the colonies of the MOLM-13 shRNA HMGN1 CDS1 in different conditions.

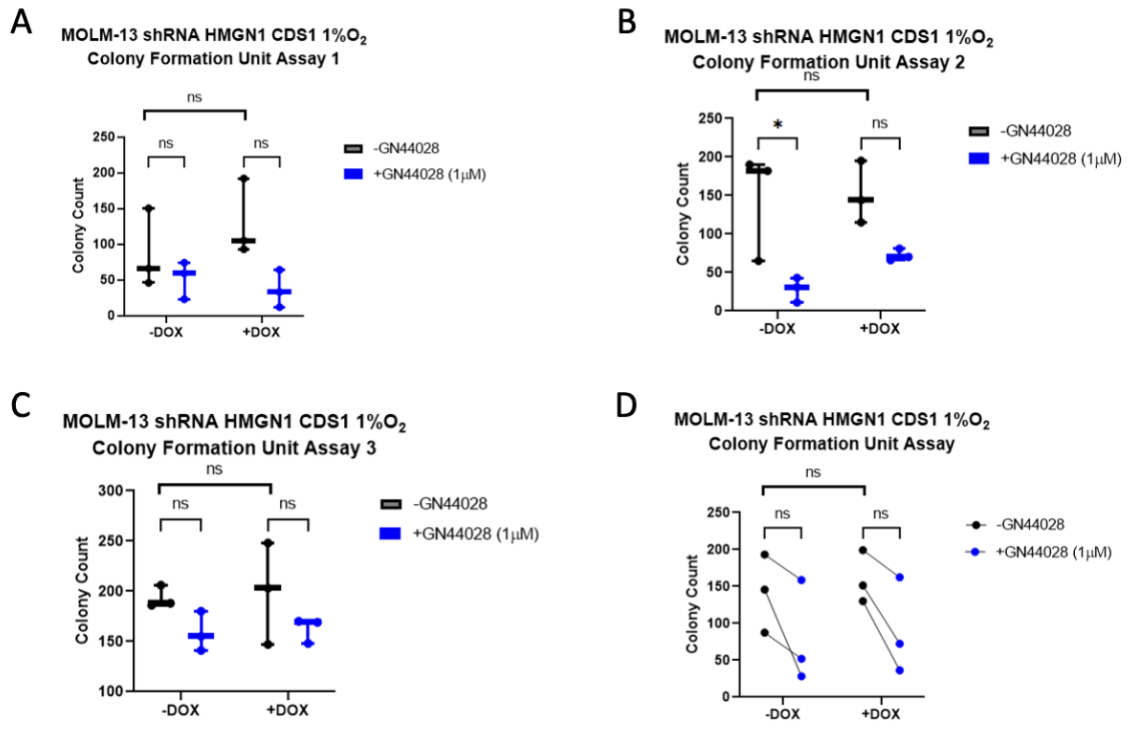

Figure 25. Colony Formation Unit assay in MOLM-13 shRNA HMGN1 CDS1 cell line. After 72hrs induction cells were seeded in their respective conditions in MethoCult at 20% with 3 technical replicates. The plates were scanned using STEMvision and images were analysed for colony count with Image J. To compare the data a two-way ANOVA test was used. n= 3. A) first biological replicate where each point is a technical replicate. B) second biological replicate. C) third biological replicate. D) Plot of the mean of each technical replicate, each dot represents a biological replicate, and the lines are to observe the trend of each experiment.

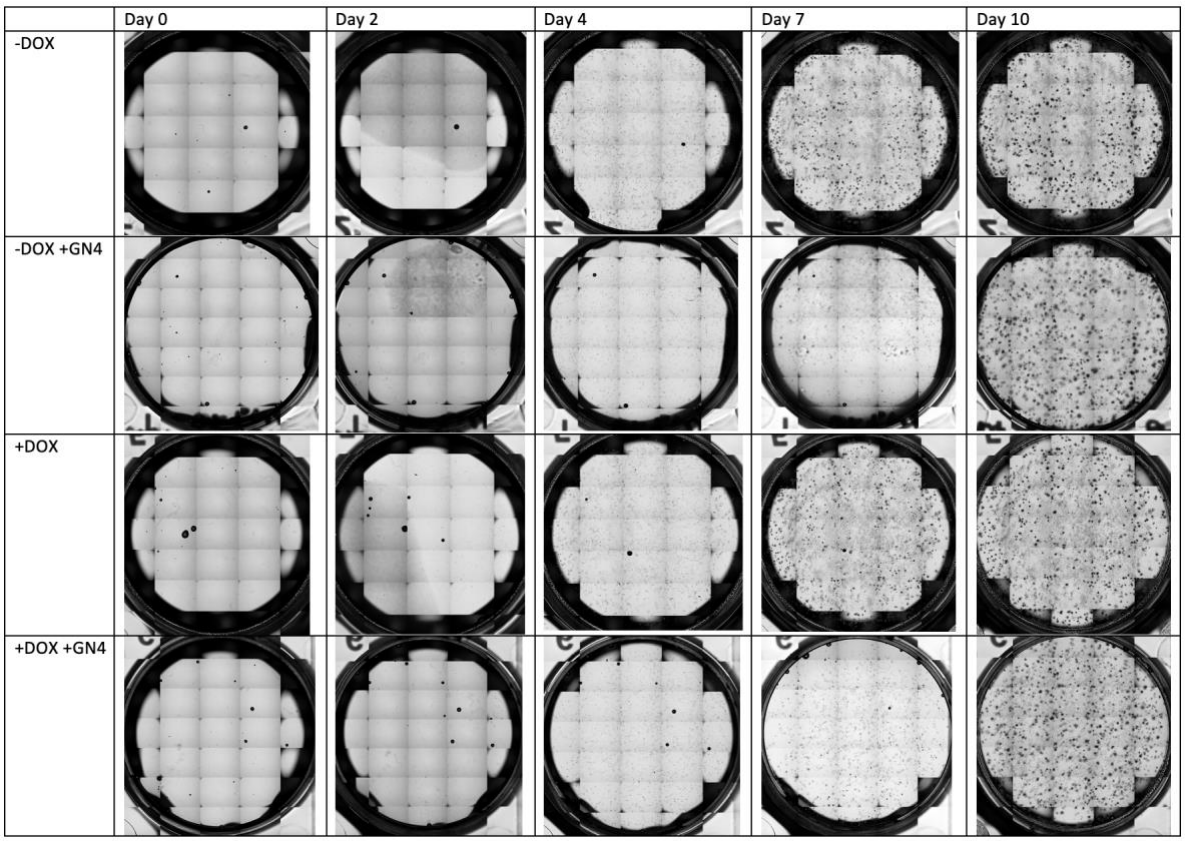

Figure 26. Representative well showing the colony formation of MOLM-13 shRNA HMGN1 CDS1 cells. Images were taken using STEMvision on day 0, day 2, day 4, day 7 and Day 10. The four conditions used can be observed: the control (-DOX) which represents no induction and no HIF-1α inhibitor, -DOX +GN4 represents the well with no HMGN1 knockdown induction but does have 1μM final concentration of the HIF-1α inhibitor GN44028. +DOX represents HMGN1 knockdown induction but no HIF-1α inhibitor. And the last condition. (+DOX +GN4) does have the HMGN1 knockdown induction and the HIF-1α inhibitor GN44028. Representative of a well of 1 replicate, n=3.

3.8 Assessing the effect of HMGN1 and HIF-1α in viability assays

Another functional assay performed was the RealTime-Glo cell viability with the HIF-1α inhibitor GN44028. This assay would assess the cell response to the change in HMGN1 expression in different oxygen-level conditions. It would also assess a more short-term effect compared to the CFU assay.

Three cell lines were assessed for cell viability using RealTime-Glo MT Cell viability a reagent that allows monitoring cell viability continuously for several days. For this assay, the cells were induced for 72hrs and after they were induced, they were set up in the plate with the respective media, RealTime Glo reagent, HIF-1α inhibitor drug and induction drug when needed.

The first cell line assessed was HL-60 shRNA HMGN1 CDS2, which was assessed in 20% O_2. When comparing the viability of the cells the time point selected to analyse was 48hrs after the HIF-1α inhibitor was added to the cells. The assay was analysed in 2 different ways: the first one is normalising to their respective 0hr treatment as seen in Figure 27A and the other is normalised to the control (no induction and no drug) at 48hrs of adding the drug as seen in Figure 28A. The first analysis allows us to observe the trend between the cells with and without the HIF-1α inhibitor and the different biological replicates. HL-60 shRNA HMGN1 CDS2 showed that there was a reduction in cell viability when GN44028 was present; however, the difference was only significant for the cells with HMGN1 knockdown (p-value= 0.0008). It also showed that the viability between the cells with and without the HMGN1 knockdown was also significant (p-value= 0.0019).

The HL-60 HMGN1 overexpression cells were assessed in normoxia (20% O_2) and hypoxia (1% O_2). In both cases, when normalised to their 0hr treatment the cells showed that there is no statistically significant difference between the viability of the samples. Though, the trend is kept in hypoxia.

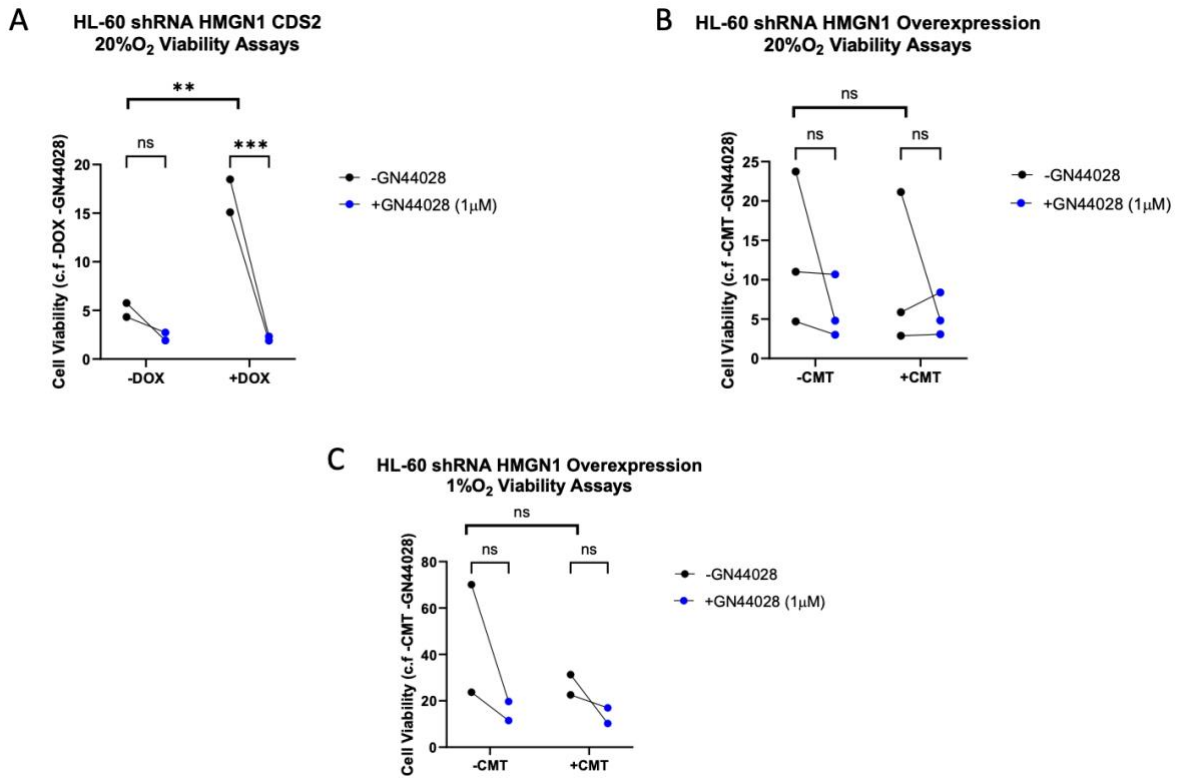

Figure 27. RealTime GLO viability assay in HL-60 HMGN1 cell lines. After 72hrs induction cells were seeded in their respective conditions including HIF-1α inhibitor GN44028 and the respective induction drug with the RealTime GLO reagents, the results were measured with CLARIOstar luminescence plate reader. Reading normalised to timepoint 0hr in drug treatment. To compare the data a two-way ANOVA test was used. A) shows the viability assay of the HL-60 shRNA HMGN1 CDS2 cell line in normoxic conditions (20% O_2). n= 2. B) shows the viability assay of the HL-60 HMGN1 overexpression cell line in normoxic conditions (20% O_2). n= 3. C) shows the viability assay of the HL-60 HMGN1 overexpression cell line in Hypoxic conditions (1% O_2). n= 2.

When the same sample set is normalised to the control (no induction and no drug) at the same time point (48hrs); the results showed that for HL-60 shRNA HMGN1 CDS2 there was no significant difference in the cell viability between conditions. Nevertheless, the p-value for the induced samples was 0.0566 with a noticeable reduction when GN44028 is present in the system. With the HL-60 shRNA HMGN1 overexpression cells incubated in normoxia (20% O_2), it showed a statistical difference between samples where in both cases the ones with the HIF-1α inhibitor was reduced for -DOX samples p-value= 0.003 and +DOX samples p-value= 0.0045. Likewise, there was a p-value of 0.0570 between the -DOX and +DOX samples without inhibitor.

For the overexpression sample in hypoxia, there was no statistical significance between the mean viability of the samples.

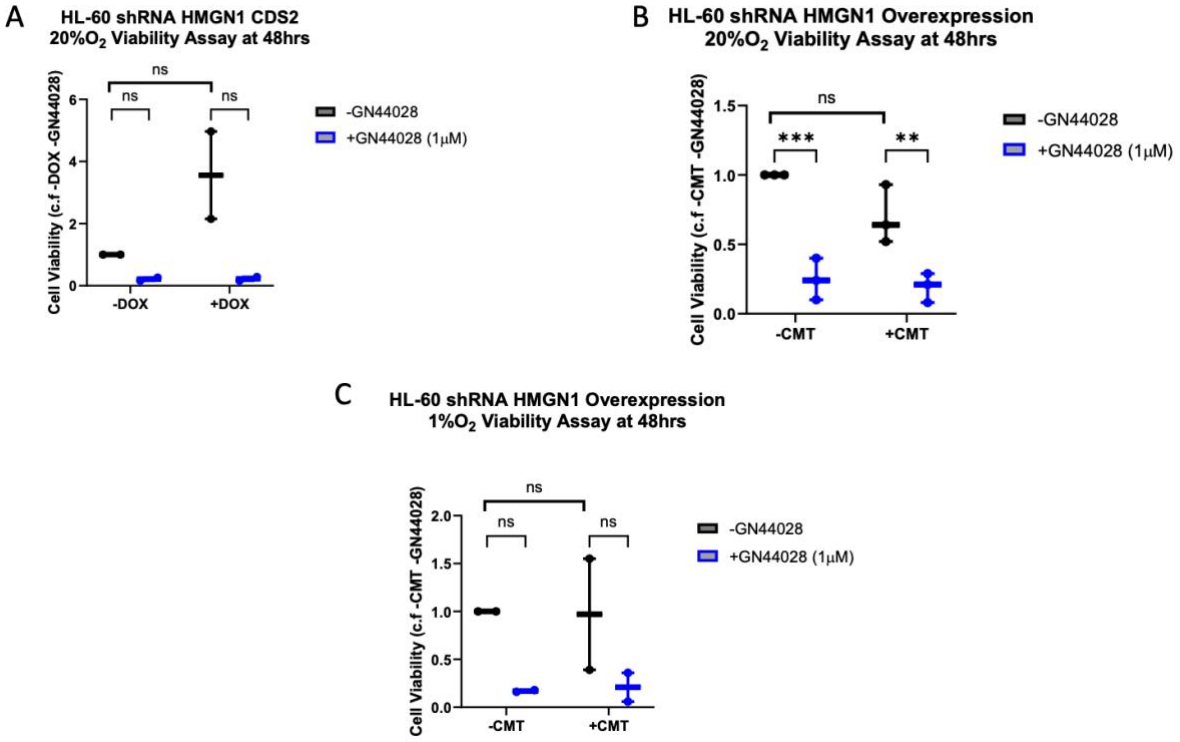

Figure 28. RealTime GLO viability assay in HL-60 HMGN1 cell lines. After 72hrs induction cells were seeded in their respective conditions including HIF-1α inhibitor GN44028 and the respective induction drug with the RealTime GLO reagents, the results were measured with CLARIOstar luminescence plate reader. Reading normalised to the control samples (no induction and no HIF-1α inhibitor) at the tested time point 48hrs. To compare the data a two-way ANOVA test was used. A) shows the viability assay of the HL-60 shRNA HMGN1 CDS2 cell line in normoxic conditions (20% O_2). n= 2. B) shows the viability assay of the HL-60 HMGN1 overexpression cell line in normoxic conditions (20% O_2). n= 3. C) shows the viability assay of the HL-60 HMGN1 overexpression cell line in Hypoxic conditions (1% O_2). n= 2.

The next cell line assessed was MOLM-13 shRNA HMGN1 CDS1, which was assessed in 1% O_2. Normalising the readings to time point 0 hr showed no statistically significant change in the cell viability. Conversely, when the luminescence readings are normalised to the control samples it showed the HIF-1α inhibitor reduces cell viability for the non-induced samples the p-value= 0.0029 and for the samples induced for knockdown the p-value= 0.0013.

MOLM-13 shRNA HMGN1 overexpression cell line was also only assessed in hypoxic conditions. This cell line showed that when analysed considering time 0hr with the inhibitor it did not show any significant result but when it was analysed at 48hrs and normalised to its control it showed a reduction in cell viability in the presence of GN44028. For the non-induced samples, the p-value= 0.0002, and for the samples induced for HMGN1 overexpression, the p-value= 0.0009.

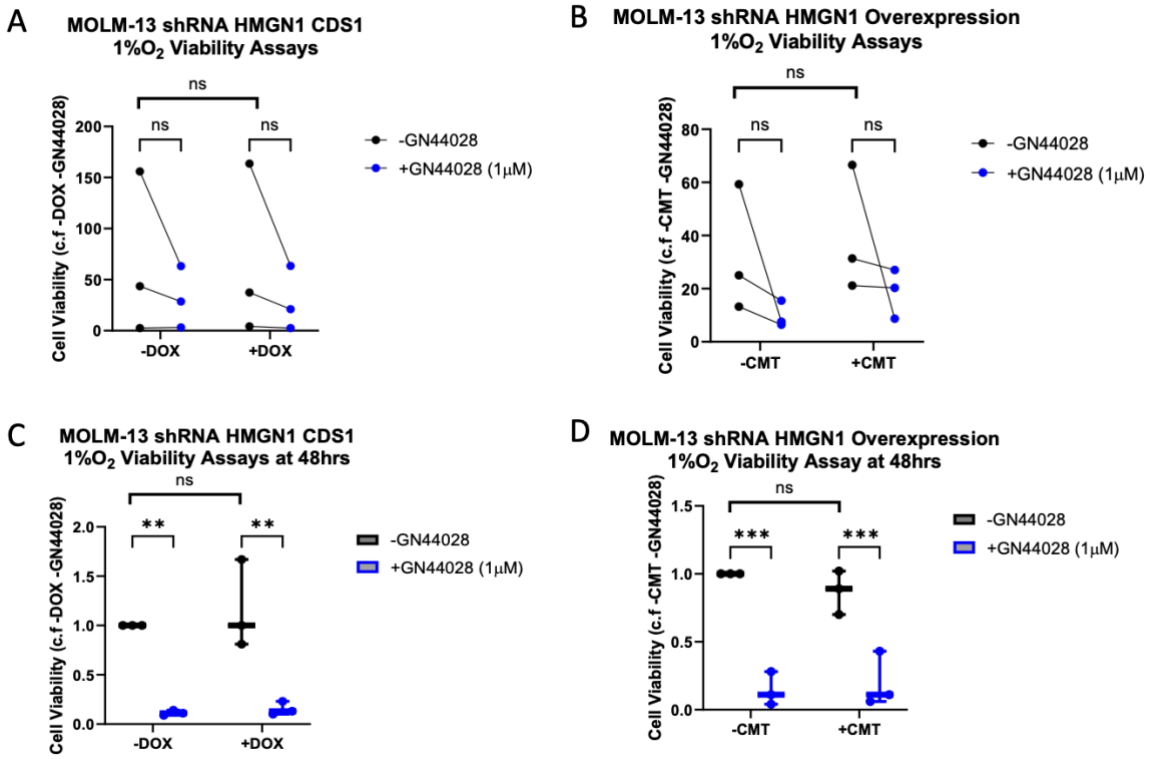

Figure 29. RealTime GLO viability assay in MOLM-13 shRNA HMGN1 cell lines. After 72hrs induction cells were seeded in their respective conditions including HIF-1α inhibitor GN44028 and the respective induction drug with the RealTime GLO reagents, the results were measured with CLARIOstar luminescence plate reader. To compare the data a two-way ANOVA test was used. A) shows the viability assay of the MOLM-13 shRNA HMGN1 CDS1 cell line, reading normalised to its time 0hr in drug treatment. B) the MOLM-13 shRNA HMGN1 overexpression cell line, reading normalised to its time 0hr in drug treatment. C) MOLM-13 shRNA HMGN1 CDS1 cell line, reading normalised to the control samples. D) shows the viability assay of the MOLM-13 shRNA HMGN1 overexpression cell line, reading normalised to the control samples. n= 3.

The last cell line assessed for viability with the GN44028 HIF-1α inhibitor was THP-1 HMGN1 overexpression. This cell line was assessed in hypoxic conditions (1% O_2). Normalising the readings to time point 0 hr showed no statistically significant change in the cell viability; however, it follows the trend of lower viability when cells are treated with the HIF-1α inhibitor. This cell line showed that when analysed at 48hrs and normalised to its control it showed a reduction in cell viability in the presence of GN44028, though not significant for the overexpressed cell line the p-value was 0.038.

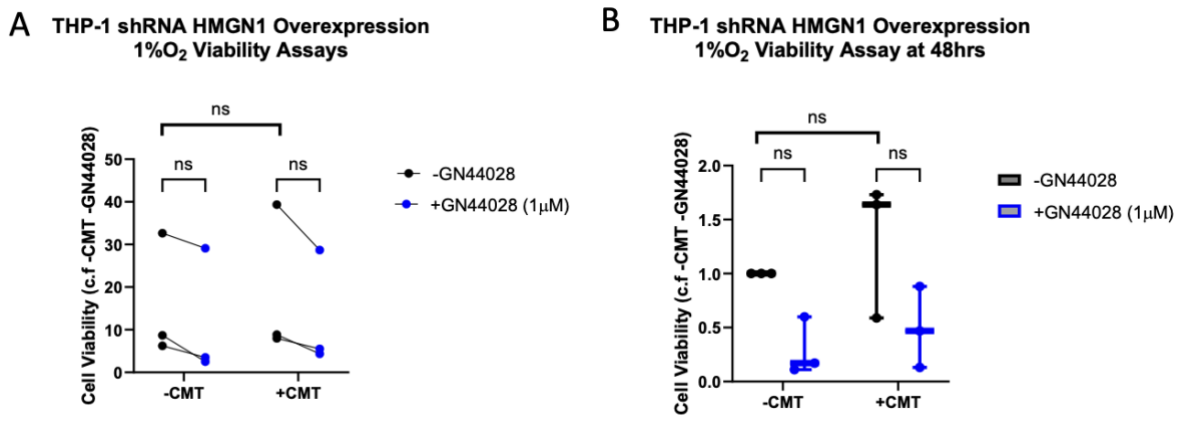

Figure 30. RealTime GLO viability assay in THP-1 HMGN1 overexpression cell line. After 72hrs induction cells were seeded in their respective conditions including HIF-1α inhibitor GN44028 and the respective induction drug with the RealTime GLO reagents, the results were measured with CLARIOstar luminescence plate reader. Two way ANOVA test was performed. A) shows the viability assay of the reading normalised to its time 0hr in drug treatment. B) shows the viability assay of the reading normalised to the control samples. n= 3.

4. Discussion

The work was focused on creating AML cell lines with HMGN1 knockdown or overexpression. The new cell lines were validated and analysed using western blots and RT-q PCR. Then to validate the mechanism of how HMGN1 can regulate HIF and understand how HIF works as an oncogenic driver in AML, three different assays were performed. First, an RT-qPCR assessing the impact of HMGN1 during hypoxia in HIF target genes where in knockdown we could see 3 different genes have been affected in the cell lines evaluated. The second and third assays were performed using a HIF-

1α inhibitor to understand the impact of HIF to promote proliferation and survival in the different HMGN1 knockdown or overexpressed cell lines.

4.1 HMGN1 expression varies over the different AML cell lines

In order to characterise the baseline levels of HMGN1 in the cell lines used in this study, western blots were performed. These assays showed a consistent trend between protein and mRNA expression; however, the cell line MOLM-13 had detectable HMGN1 mRNA whereas protein could not be detected. There are a few possible explanations for this. First, western blots were performed upon cell lines from the Bridge laboratory, whereas RNA data was sourced from proteinatlas.org [43] an open source with different RNA-seq datasets contributed from different laboratories internationally. Additionally, RNA-seq is the quantification of RNA after it had been sequenced and then counted the transcript fragments while the western blot is semi-quantitative and relied on antibodies to detect the protein [45]. This creates two different assays that cannot be compared properly between them.

Furthermore, it is well accepted in the literature [45] that RNA levels do not correlate with protein levels as there exists a delay between transcriptional induction and protein level increase. Additionally, depending on the protein it can be degraded at a different rate than it is been produced at the time of assessing the levels [45] gives a higher amount of mRNA than protein.

A future experiment to be performed is to assess the baseline mRNA and protein levels from the same sample as it would be a more robust result as the cells would be all in the same conditions and treated the same.

4.2 HMGN1 overexpression induction system might be affected by hypoxia

When assessing the induction system for HMGN1 overexpression in the different cell lines, it can be observed that in the HL-60 cell line, overexpression was observed under hypoxic conditions (Figure 13). Whereas for MOLM-13 (Figure 14) and THP-1 (Figure 15), HMGN1 overexpression was not detected. RT-qPCR performed on the

HL-60 cell line (Figure 18) similarly demonstrated a failure of HMGN1 induction when cells were exposed to hypoxia (1% O_2). Interestingly, all cell lines transduced demonstrated robust induction of HMGN1 overexpression under normoxic conditions (20% O_2) (Figures 13-15, 18). Together, these data suggest that the induction system was inhibited as a result of hypoxic treatment.

The cumate operator system was selected for this study as it has the advantage of being less toxic to cells, and can be activated in a dose-dependent manner [46]. The CMV5 promoter used by this system to express the desired construct has previously been described as hypoxia-responsive and in some studies has been shown to activate it lightly [47]. We would therefore expect that cumate induction may overexpress HMGN1 in hypoxic conditions; however, our data robustly demonstrated a failure of induction by this system under limiting oxygen. At present, there is no additional evidence that the cumate system is directly affected by hypoxia in the literature.

In light of these findings, future work should include flow cytometric analysis of transduced cell lines treated with CMT under normoxic and hypoxic conditions; an RFP reporter is contained within the CMT system, and this would demonstrate whether the lack of HMGN1 mRNA/protein under hypoxia is due to degradation of HMGN1 mRNA or inhibition of the promoter/destabilisation of CMT.

Additionally, assessing the system with DMOG, a drug that activates and stabilises HIF [48] that although not fully true to the low oxygen levels, could also help understand if the problem with the overexpression relies on the HIF-1α levels in the cells or their oxygenation status.

Another future experiment to assess HMGN1 impact on AML cell lines would be to create constitutive knockdown/ overexpression of the cell lines with paired shRNA scrambled control lines, instead of using the inducible system.

4.3 HMGN1 during hypoxic conditions does have an effect on HIF target genes

RT-qPCR analysis demonstrated that from the panel of target genes analysed, only 3 genes showed any statistically significant change upon HMGN1 knockdown. HL-60 shRNA HMGN1 cells line demonstrated reduced expression of VEGFA and CDKN1A under hypoxic conditions.

VEGFA is a growth factor that belongs to the vascular endothelial growth factor family and is considered the main stimulator of angiogenesis [49]. Among the main features of VEGFA, it is known to promote cell proliferation, vascular permeability and inhibition of apoptosis [49]. Additionally, it is known that VEGFA can be secreted by different cell types when the environment of the cells suffers from oxygen deprivation (hypoxia) as this is the main trigger for angiogenesis [49], it is even considered that VEGFA gene expression is HIF-dependant [50].

As HIF-1 is known to activate transcription of VEGFA [24,49], it was significant observing the downregulation of this gene when HMGN1 was knocked down under hypoxic conditions. Research has been performed on solid tumours as they are known to create a hypoxic environment in the middle of the tumour and need vasculature to access more oxygen [51] and it has been shown that tumour vascularization is dependent on VEGF induced by HIF-1α [52].

Nevertheless, for cancers like AML the bone marrow represents an innately hypoxic environment [24]. In the case of AML, VEGFA has been shown to bind to VEGF-R on the surface of leukaemia cells to stimulate proliferation and inhibit apoptosis [24]. Additionally, it has been found that in leukaemia even if there is no structured tumour there is evidence of increased angiogenesis in this type of cancer due to VEGF [53]. Also, it has been shown the need for hypoxia and HIF to promote proliferation and cell migration within cells of the bone marrow [54].

From the results gathered, we can suggest that in hypoxia HIF-1α will induce VEGFA transduction and HMGN1 overexpression in these cells helps HIF-1α to it. HMGN1 is known to open the chromatin for better access to the transcription factors. In AML cells

and mainly HL-60 it seems that HMGN1 does allow HIF-1α to have more access to the chromatin that usually the cells would not have; this helps cancer cells to proliferate and avoid apoptosis. Also, this showed and supported that VEGFA can be an important target for treating AML as HMGN1 showed a significant reduction of VEGFA in hypoxia and VEGFA has become essential for AML progression [24,50]

Additionally, RT-qPCR data demonstrated downregulation of CDKN1A mRNA (p21). P21 controls the G1/S phase transition in the cells [55] in part by regulating DNA damage repair and cell proliferation/death [56,57]. Furthermore, this gene has been considered to act as either a tumour suppressor or oncogene according to its localisation within the cell: in the cytoplasm, its main function is to inhibit apoptosis and promote cell migration [56].

There are certain conditions that can induce p21 expression [58] and it is known that CDKN1A is activated by HIF-1. The relationship between CDKN1A and apoptosis within the cell remains largely unclear [58]; however, it can be agreed that in cancer cells, high levels of p21 can be considered an indicator of poor response to chemotherapy and increased tumour progression [55,58].

In an assay using breast cancer cells MCF7 and U251 glioblastoma cells, Yi et al [55] showed that the upregulation of CDKN1A induced by HIF-1 can be considered a negative indicator for tumour progression. Considering that it has been suggested that in AML and mainly HL-60 cells, the upregulation of CDKN1A becomes essential for the cells to avoid apoptosis [58].

Our results showed that HMGN1 expression is also relevant for CDKN1A by allowing HIF-1α to increase CDKN1A induction when HMGN1 is overexpressed in hypoxic conditions. In HMGN1 knockdown cells, hypoxic-induced CDKN1A was downregulated meaning that the cells would not be allowed to avoid apoptosis and accumulate as it would normally do in these conditions. This opens the possibility of looking at HMGN1 expression as a therapeutic target in the future for AML.

The last gene that showed a significant difference in regulation when HMGN1 was knocked down was VLDLR. This gene was upregulated in MOLM-13 cell lines. VLDLR is a very low-density lipoprotein receptor and between its biological functions, it includes angiogenesis and tumour growth [59,60]. It has been demonstrated that hypoxia can and does increase mRNA and protein levels of VLDLR and inclusive it has been considered necessary for its induction [59].

Expression of *VLDLR* is known to be mediated by hypoxia; however, HIF/hypoxia is not the only factor that can induce its expression; it has been reported that other pathways such as PKC-ERK1/2 pathway are also able to induce the up-regulation of VLDLR in cells [61]. Additionally, this pathway has also been shown to be activated by hypoxia [62]. By knocking down HMGN1, it could be expected to down-regulate VLDLR as a HIF-1 target gene and as observed with VEGFA and CDKN1A; although, in this case, we observe an upregulation of VLDLR.

It has been shown that in AML cell lines the ERK pathway needs to be activated to promote cell survival [63], which would explain the upregulation of VLDLR as its function is to promote tumour growth. However, there is no evidence so far that HMGN1 expression is directly correlated to the ERK pathway, and it would have been expected that a direct impact of HMGN1 knockdown would inhibit the transcription of genes that promote cell proliferation and tumour growth. Nevertheless, any hypothesis of another factor impacting tumour growth in AML cells outside of HMGN1 and HIF-1α interactions would require further investigation beyond the scope of this project.

4.4 HIF-1α inhibition reveals the role of HIF-1 in proliferation in AML cell lines

GN44028 is a HIF-1α specific inhibitor [44], whose mechanism of action inhibits DNA-binding of the HIF-1α isoform. In this study, GN44028 was applied to investigate the co-operativity of HIF-1 activity with HMGN1 in AML knockdown/overexpression cell lines.

Cell viability assays demonstrated that irrespective of HMGN1 levels or oxygen conditions, treatment with GN44028 reduced cellular viability. This reflects the

importance of HIF-1 in cell proliferation as it can be observed that the effect occurred with either HMGN1 knockdown or overexpression in the different AML cell lines. Additionally, no significant effect of HMGN1 levels on viability, either by knockdown or overexpression, was observed in the AML cell lines studied in this project.

The reduced viability observed with the HIF-1α specific inhibitor demonstrated that the AML cells need HIF-1α to proliferate and survive, both under normoxic and hypoxic conditions. HIF-1 is known to regulate a wide array of genes that either promote cell proliferation or inhibit the apoptotic pathways allowing the cells to avoid death [64]. These results suggest that in these cell lines, HIF-1 may be inducing expression of genes associated with cell cycle progression/ proliferation which are repressed upon inhibition with GN44028 leading to a reduction in viability.

Additionally, the mechanism of action of GN44028 is via inhibition of HIF-1α transcriptional activity and not by reducing HIF-1α levels within the cell or the ability of HIF-1α and HIF-1β to heterodimerize in the nucleus [44]. This supports observations that the effect observed on viability is happening as a direct result of HIF-1 transcription function and target genes expressed in these cell lines. To confirm these observations, future studies focused on ascertaining the identity of HIF-1 target genes in these cell lines could be conducted, including ChIP-Seq assays, which would demonstrate where in the genome HIF-1 is binding, in the presence or absence of GN44028. These results could be confirmed by RNAseq on cells treated in the same conditions, which would indicate whether the genomic binding of HIF-1 correlated with transcript expression of the indicated target genes.

The HL-60 plates were incubated at 20% O_2 for the Colony Formation Assay to ensure induction of the CMT system for overexpression. Although it would not create a fully hypoxic environment, the effect of the HIF-1α inhibitor should be seen as the oxygen diffusion limit within the cells and tissues can travel 100-150μm from vessels to the cells [65]. In this case, the colonies would create hypoxic microenvironments whereby HIF-1 protein levels were stabilised.

HMGN1 overexpression in HL-60 cells resulted in, a significant increase in colony number compared to the non-induced HL-60s, showing HMGN1 may contribute to proliferation in this AML model. Additionally, in samples treated with the HIF-1α inhibitor, on non-induced cells, the inhibitor seems to help improve proliferation; this would indicate that HIF-1 may be performing an inhibitory role in cell proliferation in the colony-forming context, which is in contrast to its observed role in the parallel viability assays performed above. In MOLM-13 cells, the colony-forming capacity was reduced when in the presence of the HIF-1α inhibitor, which correlated with the results of the viability assay.

When comparing the results of the viability assay and the CFU assay, we can observe a greater effect on cell viability than on colony formation, due to the significant variability observed in the biological replicates of the CFU assays. In the viability results independently of HMGN1 inductions, HIF-1 inhibition decreased cell viability in all oxygen conditions. The CFU assay for HL-60 HMGN1 overexpression is the result where we can see the effect of HMGN1 on cell proliferation as the induced cells showed more colony count compared to the uninduced cells.

MOLM-13 was seeded in hypoxic conditions, allowing to ensure the most HIF-1α stable environment for the HIF-1α inhibitor. In the CFU assay, the colony count was reduced compared to the untreated: however, the HMGN1 induction did not show any significant change in cell proliferation.

To assess better these conditions in the CFU assay it would be interesting to use Pimonidazole, a hypoxic marker, to evaluate the extent of hypoxia within the colonies, which would indicate the extent of HIF-1 stabilisation and activity. Additionally, measuring colony size in addition to colony count, mainly when comparing colonies in normoxia versus hypoxia, would give further insight into the cooperativity of HIF-1/ HMGN1 in these AML cell lines.

Additionally, it would be good to assess the levels of HMGN1 after induction prior to seeding cells for the assay, and also at the end-point of the assays (48hrs for viability and 10 days for CFU). Particularly in the case of the CFU assay, which lasted 10 days,

and neither the inhibitor nor the induction drugs were topped-up in order to not disturb the colony formation. Although the induction systems should be stable during this assay, we were not able to confirm this at the endpoint due to the time limit constraints.

5. Conclusions

In conclusion, this project identified that HMGN1 can regulate HIF-1 transcription function in AML. We identify that HMGN1 levels can regulate the expression of two HIF-1 target genes, VEGFA and CDKN1A, and that inhibition of HIF-1 significantly affects the viability and colony formation of a panel of AML cell lines. These data set the stage for future studies to investigate the therapeutic potential of HIF-1 inhibition in HMGN1- overexpressing AML.

6. References

1. Pelcovits A, Niroula R. Acute Myeloid Leukemia: A Review. R I Med J [Internet]. 2020 Apr 1;103(3):38–40. Available from: https://www.ncbi.nlm.nih.gov/pubmed/32236160

2. Prada-Arismendy J, Arroyave JC, Röthlisberger S. Molecular biomarkers in acute myeloid leukemia. Blood Rev [Internet]. 2017 Jan;31(1):63–76. Available from: http://dx.doi.org/10.1016/j.blre.2016.08.005

3. De Kouchkovsky I, Abdul-Hay M. Acute myeloid leukemia: a comprehensive review and 2016 update. Blood Cancer J [Internet]. 2016 Jul 1;6(7):e441. Available from: http://dx.doi.org/10.1038/bcj.2016.50

4. Daver N, Schlenk RF, Russell NH, Levis MJ. Targeting FLT3 mutations in AML: review of current knowledge and evidence. Leukemia [Internet]. 2019 Feb;33(2):299–312. Available from: http://dx.doi.org/10.1038/s41375-018-0357-9

5. Wang R, Xu P, Chang LL, Zhang SZ, Zhu HH. Targeted therapy in NPM1-mutated AML: Knowns and unknowns. Front Oncol [Internet]. 2022 Sep 27;12:972606. Available from: http://dx.doi.org/10.3389/fonc.2022.972606

6. Daver NG, Maiti A, Kadia TM, Vyas P, Majeti R, Wei AH, et al. TP53-Mutated Myelodysplastic Syndrome and Acute Myeloid Leukemia: Biology, Current Therapy, and Future Directions. Cancer Discov [Internet]. 2022 Nov 2;12(11):2516–29. Available from: http://dx.doi.org/10.1158/2159-8290.CD-22-0332

7. Kabra A, Bushweller J. The Intrinsically Disordered Proteins MLLT3 (AF9) and MLLT1 (ENL) - Multimodal Transcriptional Switches With Roles in Normal Hematopoiesis, MLL Fusion Leukemia, and Kidney Cancer. J Mol Biol [Internet]. 2022 Jan 15;434(1):167117. Available from: http://dx.doi.org/10.1016/j.jmb.2021.167117

8. Decroocq J, Birsen R, Montersino C, Chaskar P, Mano J, Poulain L, et al. RAS activation induces synthetic lethality of MEK inhibition with mitochondrial oxidative metabolism in acute myeloid leukemia. Leukemia [Internet]. 2022 May;36(5):1237–52. Available from: http://dx.doi.org/10.1038/s41375-022-01541-0

9. You X, Liu F, Binder M, Vedder A, Lasho T, Wen Z, et al. Asxl1 loss cooperates with oncogenic Nras in mice to reprogram the immune microenvironment and drive leukemic transformation. Blood [Internet]. 2022 Feb 17;139(7):1066–79. Available from: http://dx.doi.org/10.1182/blood.2021012519

10. Ley TJ, Ding L, Walter MJ, McLellan MD, Lamprecht T, Larson DE, et al. DNMT3A mutations in acute myeloid leukemia. N Engl J Med [Internet]. 2010 Dec 16;363(25):2424–33. Available from: http://dx.doi.org/10.1056/NEJMoa1005143

11. K562 DepMap Cell Line Summary [Internet]. DepMap Portal. [cited 2023 Jan 19]. Available from: https://depmap.org/portal/cell_line/ACH-000551?tab=overview

12. HL60 DepMap Cell Line Summary [Internet]. DepMap Portal. [cited 2023 Jan 19]. Available from: https://depmap.org/portal/cell_line/ACH-000002?tab=overview

13. HL-60 [Internet]. German Collection of Microorganisms and Cell Cultures. [cited 2023 Jan 19]. Available from: https://www.dsmz.de/collection/catalogue/details/culture/ACC-3

14. MOLM13 DepMap Cell Line Summary [Internet]. DepMap Portal. [cited 2023 Jan 19]. Available from: https://depmap.org/portal/cell_line/ACH-000362?tab=overview

15. OCIAML3 DepMap Cell Line Summary [Internet]. DepMap Portal. [cited 2023 Jan 19]. Available from: https://depmap.org/portal/cell_line/ACH-000336?tab=overview

16. OCI-AML3 [Internet]. German Collection of Microorganisms and Cell Cultures. [cited 2023 Jan 19]. Available from: https://www.dsmz.de/collection/catalogue/details/culture/ACC-582

17. THP1 DepMap Cell Line Summary [Internet]. DepMap Portal. [cited 2023 Jan 19]. Available from: https://depmap.org/portal/cell_line/ACH-000146?tab=overview

18. THP-1 [Internet]. German Collection of Microorganisms and Cell Cultures. [cited 2023 Jan 19]. Available from: https://www.dsmz.de/collection/catalogue/details/culture/ACC-16

19. Dzhalilova DS, Makarova OV. HIF-Dependent Mechanisms of Relationship between Hypoxia Tolerance and Tumor Development. Biochemistry [Internet]. 2021 Oct;86(10):1163–80. Available from: http://dx.doi.org/10.1134/S0006297921100011

20. Albadari N, Deng S, Li W. The transcriptional factors HIF-1 and HIF-2 and their novel inhibitors in cancer therapy. Expert Opin Drug Discov [Internet]. 2019 Jul;14(7):667–82. Available from: http://dx.doi.org/10.1080/17460441.2019.1613370

21. Ziello JE, Jovin IS, Huang Y. Hypoxia-Inducible Factor (HIF)-1 regulatory pathway and its potential for therapeutic intervention in malignancy and ischemia. Yale J Biol Med [Internet]. 2007 Jun;80(2):51–60. Available from: https://www.ncbi.nlm.nih.gov/pubmed/18160990

22. Wang M, Chen MY, Guo XJ, Jiang JX. Expression and significance of HIF-1α and HIF-2α in pancreatic cancer. J Huazhong Univ Sci Technolog Med Sci [Internet].

2015 Dec;35(6):874–9. Available from: http://dx.doi.org/10.1007/s11596-015-1521-3

23. Fallah J, Rini BI. HIF Inhibitors: Status of Current Clinical Development. Curr Oncol Rep [Internet]. 2019 Jan 22;21(1):6. Available from: http://dx.doi.org/10.1007/s11912-019-0752-z

24. Jabari M, Allahbakhshian Farsani M, Salari S, Hamidpour M, Amiri V, Mohammadi MH. Hypoxia-Inducible Factor1-A (HIF1α) and Vascular Endothelial Growth Factor-A (VEGF-A) Expression in De Novo AML Patients. Asian Pac J Cancer Prev [Internet]. 2019 Mar 26;20(3):705–10. Available from: http://dx.doi.org/10.31557/APJCP.2019.20.3.705

25. Abdul-Aziz AM, Shafat MS, Sun Y, Marlein CR, Piddock RE, Robinson SD, et al. HIF1α drives chemokine factor pro-tumoral signaling pathways in acute myeloid leukemia. Oncogene [Internet]. 2018 May;37(20):2676–86. Available from: http://dx.doi.org/10.1038/s41388-018-0151-1

26. Migliavacca J, Percio S, Valsecchi R, Ferrero E, Spinelli A, Ponzoni M, et al. Hypoxia inducible factor-1α regulates a pro-invasive phenotype in acute monocytic leukemia. Oncotarget [Internet]. 2016 Aug 16;7(33):53540–57. Available from: http://dx.doi.org/10.18632/oncotarget.10660

27. Pias SC. Pathways of Oxygen Diffusion in Cells and Tissues : Hydrophobic Channeling via Networked Lipids. Adv Exp Med Biol [Internet]. 2020;1232:183–90. Available from: http://dx.doi.org/10.1007/978-3-030-34461-0_23

28. Nanduri R, Furusawa T, Bustin M. Biological Functions of HMGN Chromosomal Proteins. Int J Mol Sci [Internet]. 2020 Jan 10;21(2). Available from: http://dx.doi.org/10.3390/ijms21020449

29. Kugler JE, Deng T, Bustin M. The HMGN family of chromatin-binding proteins: dynamic modulators of epigenetic processes. Biochim Biophys Acta [Internet]. 2012 Jul;1819(7):652–6. Available from: http://dx.doi.org/10.1016/j.bbagrm.2012.01.013

30. Murphy KJ, Cutter AR, Fang H, Postnikov YV, Bustin M, Hayes JJ. HMGN1 and 2 remodel core and linker histone tail domains within chromatin. Nucleic Acids Res [Internet]. 2017 Sep 29;45(17):9917–30. Available from: http://dx.doi.org/10.1093/nar/gkx579

31. Lane AA, Chapuy B, Lin CY, Tivey T, Li H, Townsend EC, et al. Triplication of a 21q22 region contributes to B cell transformation through HMGN1 overexpression and loss of histone H3 Lys27 trimethylation. Nat Genet [Internet]. 2014 Jun;46(6):618–23. Available from: http://dx.doi.org/10.1038/ng.2949

32. Page EC, Heatley SL, Eadie LN, McClure BJ, de Bock CE, Omari S, et al. HMGN1 plays a significant role in CRLF2 driven Down Syndrome leukemia and provides a potential therapeutic target in this high-risk cohort. Oncogene [Internet]. 2022 Feb;41(6):797–808. Available from: http://dx.doi.org/10.1038/s41388-021-02126-4

33. Mowery CT, Reyes JM, Cabal-Hierro L, Higby KJ, Karlin KL, Wang JH, et al. Trisomy of a Down Syndrome Critical Region Globally Amplifies Transcription via HMGN1 Overexpression. Cell Rep [Internet]. 2018 Nov 13;25(7):1898-1911.e5. Available from: http://dx.doi.org/10.1016/j.celrep.2018.10.061

34. Cabal-Hierro L, van Galen P, Prado MA, Higby KJ, Togami K, Mowery CT, et al. Chromatin accessibility promotes hematopoietic and leukemia stem cell activity. Nat Commun [Internet]. 2020 Mar 16;11(1):1406. Available from: http://dx.doi.org/10.1038/s41467-020-15221-z

35. Mehnert M, Li W, Wu C, Salovska B, Liu Y. Combining rapid data independent acquisition and CRISPR gene deletion for studying potential protein functions: A case of HMGN1. Proteomics [Internet]. 2019 Jul;19(13):e1800438. Available from: https://onlinelibrary.wiley.com/doi/10.1002/pmic.201800438

36. Rochman M, Taher L, Kurahashi T, Cherukuri S, Uversky VN, Landsman D, et al. Effects of HMGN variants on the cellular transcription profile. Nucleic Acids Res [Internet]. 2011 May;39(10):4076–87. Available from: http://dx.doi.org/10.1093/nar/gkq1343

37. Page E, Heatley S, Thomas P, White D. Inducible Knockout of HMGN1 in an In Vivo xenograft Model Reduces Down Syndrome Leukemic Burden and Increases Survival Outcomes. Blood [Internet]. 2020 Nov 5 [cited 2022 Mar 3];136:25. Available from: http://www.sciencedirect.com/science/article/pii/S0006497118710756

38. Wei F, Yang D, Tewary P, Li Y, Li S, Chen X, et al. The Alarmin HMGN1 contributes to antitumor immunity and is a potent immunoadjuvant. Cancer Res [Internet]. 2014 Nov 1;74(21):5989–98. Available from: http://dx.doi.org/10.1158/0008-5472.CAN-13-2042

39. Laurent AP, Kotecha RS, Malinge S. Gain of chromosome 21 in hematological malignancies: lessons from studying leukemia in children with Down syndrome. Leukemia [Internet]. 2020 Aug;34(8):1984–99. Available from: http://dx.doi.org/10.1038/s41375-020-0854-5

40. Lee P, Bhansali R, Izraeli S, Hijiya N, Crispino JD. The biology, pathogenesis and clinical aspects of acute lymphoblastic leukemia in children with Down syndrome. Leukemia [Internet]. 2016 Sep;30(9):1816–23. Available from: http://dx.doi.org/10.1038/leu.2016.164

41. Wee S, Wiederschain D, Maira SM, Loo A, Miller C, deBeaumont R, et al. PTEN-deficient cancers depend on PIK3CB. Proc Natl Acad Sci U S A [Internet]. 2008 Sep 2;105(35):13057–62. Available from: http://dx.doi.org/10.1073/pnas.0802655105

42. Wiederschain D, Wee S, Chen L, Loo A, Yang G, Huang A, et al. Single-vector inducible lentiviral RNAi system for oncology target validation. Cell Cycle [Internet]. 2009 Feb 1;8(3):498–504. Available from: http://dx.doi.org/10.4161/cc.8.3.7701

43. Cell line - HMGN1 - The Human Protein Atlas [Internet]. [cited 2023 Mar 30]. Available from: https://www.proteinatlas.org/ENSG00000205581-HMGN1/cell+line

44. Minegishi H, Fukashiro S, Ban HS, Nakamura H. Discovery of Indenopyrazoles as a New Class of Hypoxia Inducible Factor (HIF)-1 Inhibitors. ACS Med Chem Lett [Internet]. 2013 Feb 14;4(2):297–301. Available from: http://dx.doi.org/10.1021/ml3004632

45. Liu Y, Beyer A, Aebersold R. On the Dependency of Cellular Protein Levels on mRNA Abundance. Cell [Internet]. 2016 Apr 21;165(3):535–50. Available from: http://dx.doi.org/10.1016/j.cell.2016.03.014

46. Mullick A, Xu Y, Warren R, Koutroumanis M, Guilbault C, Broussau S, et al. The cumate gene-switch: a system for regulated expression in mammalian cells. BMC Biotechnol [Internet]. 2006 Nov 3;6:43. Available from: http://dx.doi.org/10.1186/1472-6750-6-43

47. Wendland K, Thielke M, Meisel A, Mergenthaler P. Intrinsic hypoxia sensitivity of the cytomegalovirus promoter. Cell Death Dis [Internet]. 2015 Oct 15;6(10):e1905. Available from: http://dx.doi.org/10.1038/cddis.2015.259

48. Zhdanov AV, Okkelman IA, Collins FWJ, Melgar S, Papkovsky DB. A novel effect of DMOG on cell metabolism: direct inhibition of mitochondrial function precedes HIF target gene expression. Biochim Biophys Acta [Internet]. 2015 Oct;1847(10):1254–66. Available from: http://dx.doi.org/10.1016/j.bbabio.2015.06.016

49. Melincovici CS, Boşca AB, Şuşman S, Mărginean M, Mihu C, Istrate M, et al. Vascular endothelial growth factor (VEGF) - key factor in normal and pathological angiogenesis. Rom J Morphol Embryol [Internet]. 2018;59(2):455–67. Available from: https://www.ncbi.nlm.nih.gov/pubmed/30173249

50. Hoseinkhani Z, Rastegari-Pouyani M, Oubari F, Mozafari H, Rahimzadeh AB, Maleki A, et al. Contribution and prognostic value of TSGA10 gene expression in patients with acute myeloid leukemia (AML). Pathol Res Pract [Internet]. 2019 Mar;215(3):506–11. Available from: http://dx.doi.org/10.1016/j.prp.2019.01.003

51. Li L, Rispoli R, Patient R, Ciau-Uitz A, Porcher C. Etv6 activates vegfa expression through positive and negative transcriptional regulatory networks in Xenopus

embryos. Nat Commun [Internet]. 2019 Mar 6;10(1):1083. Available from: http://dx.doi.org/10.1038/s41467-019-09050-y

52. Carmeliet P, Dor Y, Herbert JM, Fukumura D, Brusselmans K, Dewerchin M, et al. Role of HIF-1alpha in hypoxia-mediated apoptosis, cell proliferation and tumour angiogenesis. Nature [Internet]. 1998 Jul 30;394(6692):485–90. Available from: http://dx.doi.org/10.1038/28867

53. Mohammadi Najafabadi M, Shamsasenjan K, Akbarzadehalaleh P. Angiogenesis Status in Patients with Acute Myeloid Leukemia: From Diagnosis to Post-hematopoietic Stem Cell Transplantation. Int J Organ Transplant Med [Internet]. 2017 May 1;8(2):57–67. Available from: https://www.ncbi.nlm.nih.gov/pubmed/28828165

54. Archacka K, Grabowska I, Mierzejewski B, Graffstein J, Górzyńska A, Krawczyk M, et al. Hypoxia preconditioned bone marrow-derived mesenchymal stromal/stem cells enhance myoblast fusion and skeletal muscle regeneration. Stem Cell Res Ther [Internet]. 2021 Aug 9;12(1):448. Available from: http://dx.doi.org/10.1186/s13287-021-02530-3

55. Yi L, Lin X, Li H, Ma Y, Lin JM. Dynamic imaging of MYC and CDKN1A mRNAs as an indicator of cell G1-phase arrest. Chem Commun [Internet]. 2017 Feb 2;53(11):1900–3. Available from: http://dx.doi.org/10.1039/c6cc10078c

56. Dutto I, Tillhon M, Cazzalini O, Stivala LA, Prosperi E. Biology of the cell cycle inhibitor p21(CDKN1A): molecular mechanisms and relevance in chemical toxicology. Arch Toxicol [Internet]. 2015 Feb;89(2):155–78. Available from: http://dx.doi.org/10.1007/s00204-014-1430-4

57. Jeon BN, Kim MK, Choi WI, Koh DI, Hong SY, Kim KS, et al. KR-POK interacts with p53 and represses its ability to activate transcription of p21WAF1/CDKN1A. Cancer Res [Internet]. 2012 Mar 1;72(5):1137–48. Available from: http://dx.doi.org/10.1158/0008-5472.CAN-11-2433

58. Freemerman AJ, Vrana JA, Tombes RM, Jiang H, Chellappan SP, Fisher PB, et al. Effects of antisense p21 (WAF1/CIP1/MDA6) expression on the induction of

differentiation and drug-mediated apoptosis in human myeloid leukemia cells (HL-60). Leukemia [Internet]. 1997 Apr;11(4):504–13. Available from: http://dx.doi.org/10.1038/sj.leu.2400625

59. Yang D, Gao L, Wang T, Qiao Z, Liang Y, Zhang P. Hypoxia triggers endothelial endoplasmic reticulum stress and apoptosis via induction of VLDL receptor. FEBS Lett [Internet]. 2014 Nov 28;588(23):4448–56. Available from: http://dx.doi.org/10.1016/j.febslet.2014.09.046

60. Takahashi S, Sakai J, Fujino T, Hattori H, Zenimaru Y, Suzuki J, et al. The very low-density lipoprotein (VLDL) receptor: characterization and functions as a peripheral lipoprotein receptor. J Atheroscler Thromb [Internet]. 2004;11(4):200–8. Available from: http://dx.doi.org/10.5551/jat.11.200

61. Liu Z, Li H, Li Y, Wang Y, Zong Y, Feng Y, et al. Up-regulation of VLDL receptor expression and its signaling pathway induced by VLDL and β-VLDL. J Huazhong Univ Sci Technolog Med Sci [Internet]. 2009 Feb 1;29(1):1–7. Available from: https://doi.org/10.1007/s11596-009-0101-9

62. Minet E, Arnould T, Michel G, Roland I, Mottet D, Raes M, et al. ERK activation upon hypoxia: involvement in HIF-1 activation. FEBS Lett [Internet]. 2000 Feb 18;468(1):53–8. Available from: http://dx.doi.org/10.1016/s0014-5793(00)01181-9

63. Su Y, Li X, Ma J, Zhao J, Liu S, Wang G, et al. Targeting PI3K, mTOR, ERK, and Bcl-2 signaling network shows superior antileukemic activity against AML ex vivo. Biochem Pharmacol [Internet]. 2018 Feb;148:13–26. Available from: http://dx.doi.org/10.1016/j.bcp.2017.11.022

64. Muz B, de la Puente P, Azab F, Azab AK. The role of hypoxia in cancer progression, angiogenesis, metastasis, and resistance to therapy. Hypoxia (Auckl) [Internet]. 2015 Dec 11;3:83–92. Available from: http://dx.doi.org/10.2147/HP.S93413

65. Pires IM, Bencokova Z, Milani M, Folkes LK, Li JL, Stratford MR, et al. Effects of acute versus chronic hypoxia on DNA damage responses and genomic instability.

Cancer Res [Internet]. 2010 Feb 1;70(3):925–35. Available from: http://dx.doi.org/10.1158/0008-5472.CAN-09-2715

66. pCDH-CuO-MCS-EF1α-RFP+Puro SparQ™ Cloning and Expression Lentivector [Internet]. System Biosciences, LLC; [cited 2022 Oct 18]. Available from: https://www.systembio.com/products/gene-expression-systems/cumate-inducible-systems/cumate-inducible-cloning-and-expression-vector/pcdh-cuo-mcs-ef1-rfp-puro-sparq-cloning-and-expression-lentivector

67. Addgene: Tet-pLKO-puro [Internet]. [cited 2023 Apr 13]. Available from: https://www.addgene.org/21915/

7. Appendix

Appendix 1. Plasmid vector map for HMGN1 overexpression using Cumate as promoter switch and using puromycin and RFP tag for selection [66].

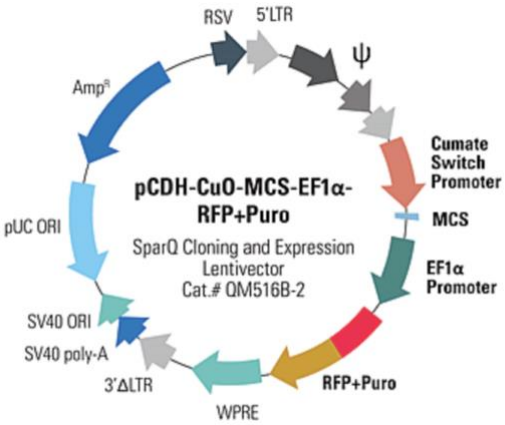

Appendix 2. Plasmid vector map for shRNA HMGN1 knockdown using Doxycycline as promoter switch and puromycin for selection [67].

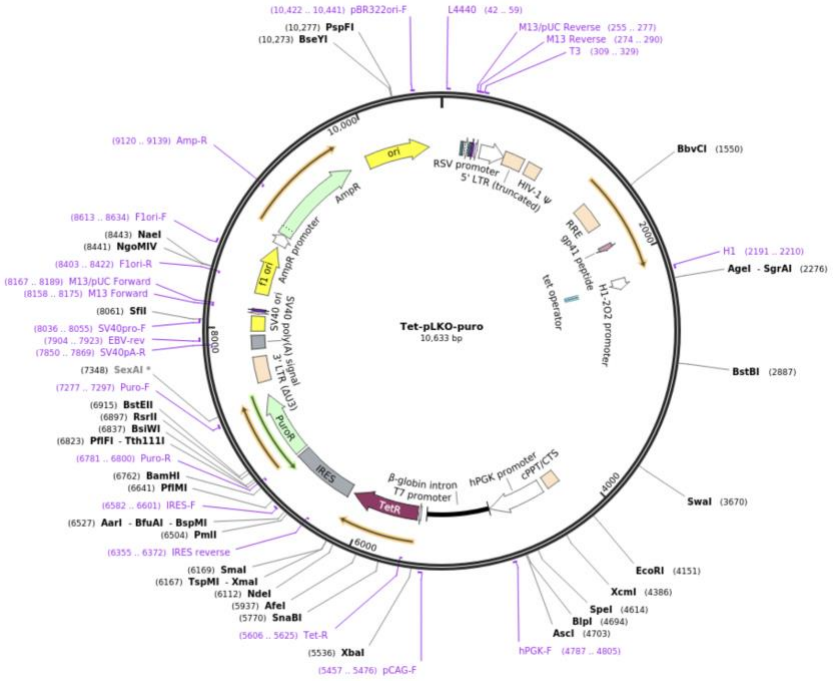

Appendix 3. cDNA sequence of human HMGN1. Text highlighted in red and green indicates the coding sequence regions targeted by two different shRNAs: coding sequence 1 (CDS1) and coding sequence 2 (CDS2), respectively. The start codon (ATG) is indicated in blue, and the stop codon (TAA) is orange.

ATGCCCAAGAGGAAGGTCAGCTCCGCCGAAGGCGCCGCCAAGGAAGAGCCCAAGAGGAGATCGGCGCG
GTTGTCAGCTAAACCTCCTGCAAAAGTGGAAGCGAAGCCGAAAAAGGCAGCAGC**GAAGGATAAATCTT**
CAGACAAAAAAGTGCAAACAAAAGGGAAAAGGGGAGCAAAGGGAAAACAGGCCGAAGTGGCTAA**CCAA**
GAAACTAAAGAAGACTTACCTGCGGAAAACGGGGAAACGAAGACTGAGGAGAGTCCAGCCTCTGATGA
AGCAGGAGAGAAAGAAGCCAAGTCTGATTAA.

Appendix 4. Figure showing the time course progression of the HMGN1 overexpression in the HL-60 cell line. Taken by fluorescent microscopy during CFU assay.

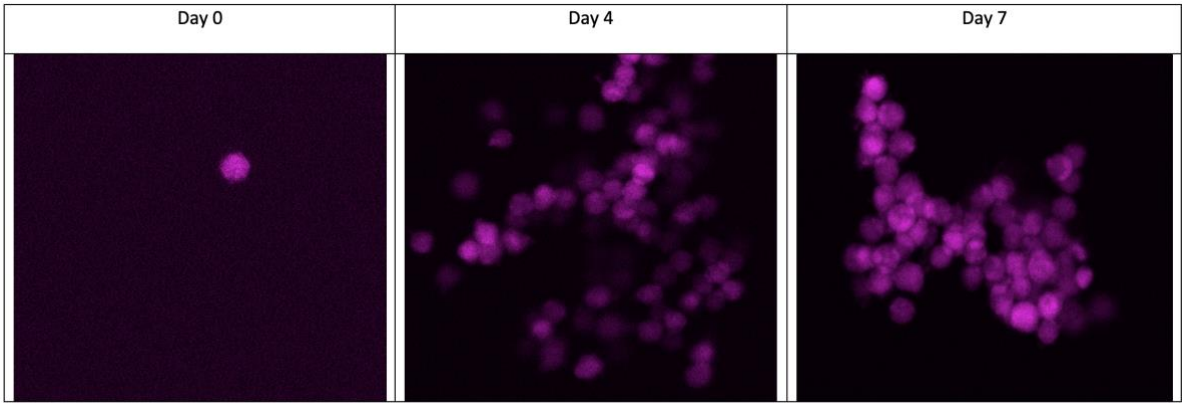

Appendix 5. Figure showing the result of n=1, ChIP-qPCR assay.